

# Attack-Aware Noise Calibration for Differential Privacy

Bogdan Kulynych<sup>\*1,2</sup>, Juan Felipe Gomez<sup>\*3</sup>,  
Georgios Kaissis<sup>4</sup>, Flavio du Pin Calmon<sup>3</sup>, and Carmela Troncoso<sup>5</sup>

<sup>1</sup>Lausanne University Hospital (CHUV)

<sup>2</sup>University of Lausanne

<sup>3</sup>Harvard University

<sup>4</sup>Technical University Munich

<sup>5</sup>EPFL

## Abstract

Differential privacy (DP) is a widely used approach for mitigating privacy risks when training machine learning models on sensitive data. DP mechanisms add noise during training to limit the risk of information leakage. The scale of the added noise is critical, as it determines the trade-off between privacy and utility. The standard practice is to select the noise scale in terms of a *privacy budget parameter*  $\epsilon$ . This parameter is in turn interpreted in terms of operational *attack risk*, such as accuracy, or sensitivity and specificity of inference attacks against the privacy of the data. We demonstrate that this two-step procedure of first calibrating the noise scale to a privacy budget  $\epsilon$ , and then translating  $\epsilon$  to attack risk leads to overly conservative risk assessments and unnecessarily low utility. We propose methods to directly calibrate the noise scale to a desired attack risk level, bypassing the intermediate step of choosing  $\epsilon$ . For a target attack risk, our approach significantly decreases noise scale, leading to increased utility at the same level of privacy. We empirically demonstrate that calibrating noise to attack sensitivity/specificity, rather than  $\epsilon$ , when training privacy-preserving ML models substantially improves model accuracy for the same risk level. Our work provides a principled and practical way to improve the utility of privacy-preserving ML without compromising on privacy.

## 1 Introduction

Machine learning and statistical models can leak information about individuals in their training data, which can be recovered by membership inference, attribute inference, and reconstruction attacks (Fredrikson et al., 2015; Shokri et al., 2017; Yeom et al., 2018; Balle et al., 2022b). The most common defenses against these attacks are based on differential privacy (DP) (Dwork et al., 2014). Differential privacy introduces noise to either the data, the training algorithm, or the model parameters (Chaudhuri et al., 2011). This noise provably limits the adversary’s ability to run successful privacy attacks at the cost of reducing the utility of the model.

In DP, two parameters  $\epsilon$  and  $\delta$  control the privacy-utility trade-off by determining the scale (e.g., variance) of the noise added during training. Smaller values of these parameters correspond to larger noise. Larger noise provides stronger privacy guarantees but reduces the utility of the trained model. Typically,  $\delta$  is set to a small fixed value (usually between  $10^{-8}$  and  $10^{-5}$ ), leaving  $\epsilon$  as the primary tunable parameter. Without additional analysis, the parameters  $(\epsilon, \delta)$  alone do not provide a tangible and intuitive operational notion of privacy risk (Nanayakkara et al., 2023). This begs the question: how should practitioners, regulators, and data subjects decide on acceptable values of  $\epsilon$  and  $\delta$  and calibrate the noise scale to achieve a desired level of protection?

A standard way of assigning operational meaning to DP parameters is mapping them to *attack risks*. One common approach is computing the maximum accuracy (equivalently, advantage) of membership inference attacks that  $(\epsilon, \delta)$  allows (Wood et al., 2018). An alternative is to compute the trade-off curve between sensitivity and specificity of feasible membership inference attacks (Dong et al., 2022), which was recently shown to be directly related to success rates of record reconstruction attacks (Hayes et al., 2024; Kaissis et al., 2023a). All these analyses map  $(\epsilon, \delta)$  to a quantifiable level of risk for individuals whose data is present in the dataset. Studies

---

\*Contributed equally.

Direct calibration of noise to attack risk increases test accuracy compared to the standard calibration at the same level of risk:

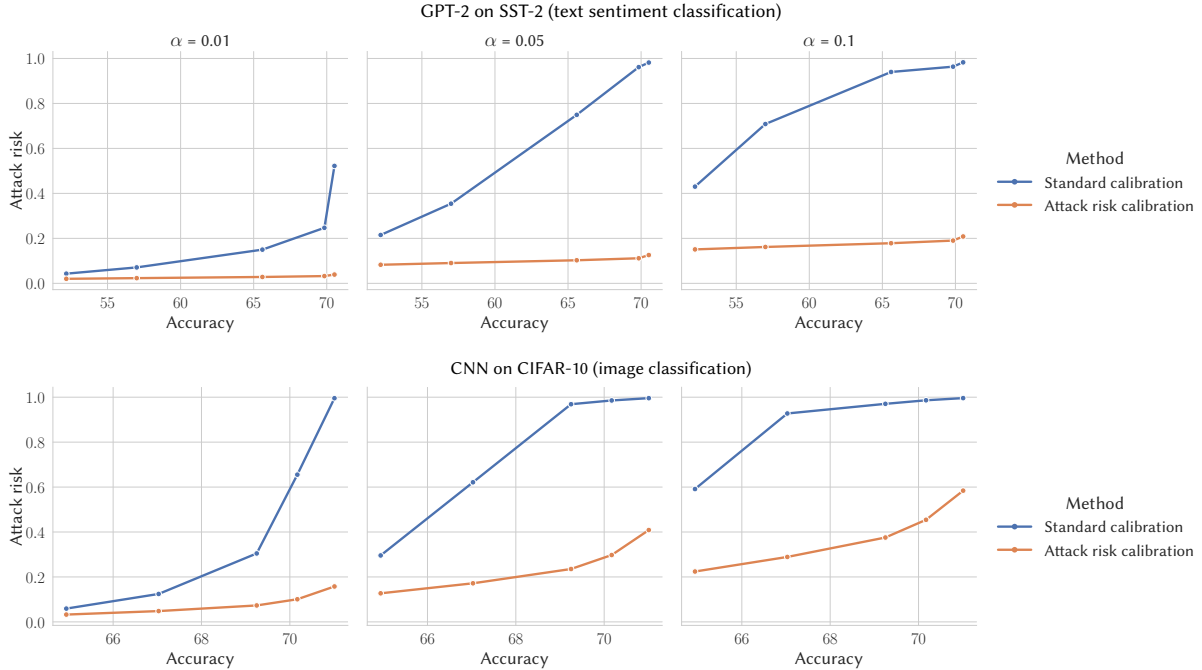


**Figure 1:** The plots show test accuracy (x-axis) of a privately finetuned GPT-2 on SST-2 text sentiment classification dataset (top) and a convolutional neural network on CIFAR-10 image classification dataset (bottom). The DP noise is calibrated to guarantee at most a certain level of privacy attack sensitivity (y-axis) at three possible attack false-positive rates  $\alpha \in \{0.01, 0.05, 0.1\}$ . See Section 4 for details.

have shown that risk-based measures like these are the most useful way to interpret the guarantees afforded by DP for practitioners and data subjects (Cummings et al., 2021; Franzen et al., 2022; Nanayakkara et al., 2023).

In this work, we show that directly calibrating the level of noise to satisfy a given level of attack risk, as opposed to satisfying a certain  $\epsilon$ , enables a significant increase in utility (see Figure 1). We enable this direct calibration to attack risk by working under  $f$ -DP (Dong et al., 2022), a hypothesis testing interpretation of DP. In particular, we extend the tight privacy analysis method by Doroshenko et al. (2022), which uses  $(\epsilon, \delta)$ -DP, to directly estimate operational privacy risk notions in  $f$ -DP, and use this algorithm to directly calibrate the level of noise to satisfy a given level of attack risk. Concretely, our contributions are:

1. We provide efficient methods for calibrating noise to (a) maximum accuracy (equivalently, advantage), (b) sensitivity and specificity of membership inference attacks, in any DP mechanism, including DP-SGD (Abadi et al., 2016) with arbitrarily many steps.
2. We empirically show that our calibration methods reduce the required noise scale for a given level of privacy risk, up to  $2\times$  as compared to standard methods for choosing DP parameters. In a private language modeling task with GPT-2 (Radford et al., 2019), we demonstrate that the decrease in noise translates to an up to 18 p.p. gain in classification accuracy.
3. We demonstrate that relying on membership inference accuracy as an interpretation of privacy risk, as is common practice, can increase attack power in security-critical regimes, and that calibration for sensitivity and specificity does not suffer from this drawback.
4. We provide an easy-to-use Python package which implements our calibration methods.<sup>†</sup>

Ultimately, we advocate for practitioners to calibrate the noise level in privacy-preserving machine learning algorithms to a sensitivity and specificity constraint under  $f$ -DP as outlined in Section 3.2.

**Related Work.** Prior work has studied methods for communicating the privacy guarantees afforded by differential privacy (Nanayakkara et al., 2023, 2022; Franzen et al., 2022; Mehner et al., 2021; Wood et al., 2018), and

<sup>†</sup>[github.com/bogdan-kulynych/riskcal](https://github.com/bogdan-kulynych/riskcal)

introduced various principled methods for choosing the privacy parameters (Abowd and Schmutte, 2015; Nissim et al., 2014; Hsu et al., 2014). Unlike our approach, these works assume that the mechanisms are calibrated to a given  $\varepsilon$  privacy budget parameter, and do not aim to directly set the privacy guarantees in terms of operational notions of privacy risk.

Cherubin et al. (2024); Ghazi and Issa (2023); Izzo et al. (2022); Mahloujifar et al. (2022) use variants of DP that directly limit the advantage of membership inference attacks. We show that calibrating noise to a given level of advantage can increase privacy risk in security-critical regimes and provide methods that mitigate this issue. Leemann et al. (2024) provide methods for evaluating the success of membership inference attacks under a weaker threat model than in DP. Unlike their work, we preserve the standard strong threat model in differential privacy but set and report the privacy guarantees in terms of an operational notion of risk under  $f$ -DP as opposed to the  $\varepsilon$  parameter.

## 2 Problem Statement

### 2.1 Preliminaries

**Setup and notation.** Let  $\mathbb{D}^n$  denote the set of all datasets of size  $n$  over a space  $\mathbb{D}$ , and let  $S \simeq S'$  denote a neighboring relation, e.g. that  $S, S'$  differ by one datapoint. We study randomized algorithms (*mechanisms*)  $M(S)$  that take as input a dataset  $S \in \mathbb{D}^n$ , and output the result of a computation, e.g., statistical queries or an ML model. We denote the output domain of the mechanism by  $\Theta$ . For ease of presentation, we mainly consider randomized mechanisms that are parameterized by a single noise parameter  $\omega \in \Omega$ , but our results extend to mechanisms with multiple parameters. For example, in the *Gaussian mechanism* (Dwork et al., 2014),  $M(S) = q(S) + Z$ , where  $Z \sim \mathcal{N}(0, \sigma^2)$  and  $q(S)$  is a non-private statistical algorithm, the parameter is  $\omega = \sigma$  with  $\Omega = \mathbb{R}^+$ . We denote a parameterized mechanism by  $M_\omega(S)$ .

**Differential Privacy.** For any  $\gamma \geq 0$ , we define the hockey-stick divergence from distribution  $P$  to  $Q$  over a domain  $\mathcal{O}$  by

$$D_\gamma(P \parallel Q) \triangleq \sup_E P(E) - \gamma Q(E) \quad (1)$$

where the supremum is taken over all measurable sets  $E \subseteq \mathcal{O}$ . We define differential privacy (DP) (Dwork et al., 2006) as follows:

**Definition 2.1.** A mechanism  $M(\cdot)$  satisfies  $(\varepsilon, \delta)$ -DP iff for all  $S \simeq S'$ ,  $D_{e^\varepsilon}(M(S), M(S')) \leq \delta$ .

Lower values of  $\varepsilon$  and  $\delta$  mean more privacy, and vice versa. In the rest of the paper we assume w.l.o.g. that larger value of the parameter  $\omega$  means that the mechanism  $M_\omega(\cdot)$  is more noisy, which translates into higher level of privacy (smaller  $\varepsilon, \delta$ ), but lower utility.

Most DP algorithms satisfy a collection of  $(\varepsilon, \delta)$ -DP guarantees. We define the *privacy profile* (Balle and Wang, 2018), or *privacy curve* (Gopi et al., 2021; Alghamdi et al., 2022) of a mechanism as:

**Definition 2.2.** A parameterized mechanism  $M_\omega(\cdot)$  has a privacy profile  $\varepsilon_\omega : \mathbb{R} \rightarrow [0, 1]$  if for every  $\delta \in [0, 1]$ ,  $M_\omega(\cdot)$  is  $(\varepsilon(\delta), \delta)$ -DP.

In a slight abuse of notation, we refer to the function  $\delta_\omega(\varepsilon)$ , defined analogously, also as the privacy profile.

**DP-SGD.** A common algorithm for training neural networks with DP guarantees is DP-SGD (Abadi et al., 2016). The basic building block of DP-SGD is the so-called *subsampled Gaussian mechanism*, defined as  $M(S) = q(\text{PoissonSample}_p S) + Z$ , where  $Z \sim \mathcal{N}(0, \Delta_2^2 \cdot \sigma^2 \cdot I_d)$ , and  $\text{PoissonSample}_p$  is a procedure which subsamples a dataset  $S$  such that every record has the same probability  $p \in (0, 1)$  to be in the subsample. DP-SGD, parameterized by  $p, \sigma$ , and  $T \geq 1$ , is a repeated application of the subsampled Gaussian mechanism:  $M^{(1)} \circ M^{(2)} \circ \dots \circ M^{(T)}(S)$ , where  $q^{(i)}(\cdot)$  is a single step of gradient descent with per-record gradient clipping to  $\Delta_2$  Euclidean norm. In line with a standard practice (Ponomareva et al., 2023), we regard all parameters but  $\sigma$  as fixed, thus  $\omega = \sigma$ .

Privacy profiles for mechanisms such as DP-SGD are computed via numerical algorithms called *accountants* (see, e.g., Abadi et al., 2016; Gopi et al., 2021; Doroshenko et al., 2022; Alghamdi et al., 2022). These algorithms compute the achievable privacy profile to accuracy nearly matching the lower bound of a privacy audit where the adversary is free to choose the entire (pathological or realistic) training dataset (Nasr et al., 2021, 2023). Given these results, we regard the analysis of these accountants as tight, and use them for calibration to a particular  $(\varepsilon, \delta)$ -DP constraint.

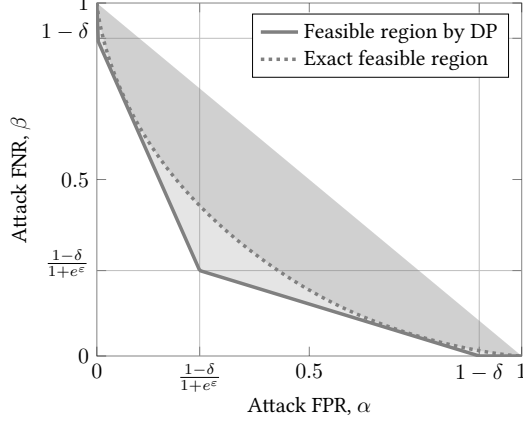


**Figure 2:** Trade-off curves of a Gaussian mechanism that satisfies  $(\varepsilon, \delta)$ -DP. Each curve shows a boundary of the feasible region (greyed out) of possible membership inference attack FPR ( $\alpha$ ) and FNR ( $\beta$ ) pairs. The solid curve shows the limit of the feasible region guaranteed by DP via Eq. (5), which is a conservative overestimate of attack success rates compared to the exact trade-off curve (dotted). The maximum advantage  $\eta$  is achieved with FPR and FNR at the point closest to the origin.

**Standard Calibration.** The procedure of choosing the parameter  $\omega \in \Omega$  to satisfy a given level of privacy is called *calibration*. In *standard calibration*, one chooses  $\omega$  given a target DP guarantee  $\varepsilon^*$  and an accountant that supplies a privacy profile  $\varepsilon_\omega(\delta)$  for any noise parameter  $\omega \in \Omega$ , to ensure that  $M_\omega(S)$  satisfies  $(\varepsilon^*, \delta^*)$ -DP:

$$\min_{\omega \in \Omega} \omega \quad \text{s.t.} \quad \varepsilon_\omega(\delta^*) \geq \varepsilon^*, \quad (2)$$

with  $\delta^*$  set by convention to  $\delta^* = 1/c \cdot n$ , where  $n$  is the dataset size, and  $c > 1$  (see, e.g., Ponomareva et al., 2023). The parameter  $\varepsilon^*$  is also commonly chosen by convention between 3 and 10 for privacy-persevering ML algorithms with practical utility (Ponomareva et al., 2023; Sander et al., 2023; De et al., 2022; Wutschitz et al., 2022). In Eq. (2) and the rest of the paper we denote by  $*$  the target value of privacy risk.

After calibration, the  $(\varepsilon^*, \delta^*)$  parameters are often mapped to some operational notation of privacy attack risk for interpretability. In the next section, we introduce the hypothesis testing framework of DP,  $f$ -DP, and the notions of risk that  $(\varepsilon, \delta)$  parameters are often mapped to. In contrast to standard calibration, in Section 2.3, we calibrate  $\omega$  to minimize these privacy risks.

## 2.2 Operational Privacy Risks

It is possible to interpret differential privacy entirely through the lens of membership inference attacks (MIAs) in the so-called *strong adversary model* (see, e.g., Nasr et al., 2021). In this framework, the adversary aims to determine whether a given output  $\theta \in \Theta$  came from  $M(S)$  or  $M(S')$ , where  $S' = S \cup \{z\}$  for some target example  $z \in \mathbb{D}$ . The adversary has access to the mechanism  $M(\cdot)$ , the dataset  $S$ , and the target example  $z \in \mathbb{D}$ . Such an attack is equivalent to a binary hypothesis test (Wasserman and Zhou, 2010; Kairouz et al., 2015; Dong et al., 2022):

$$H_0 : \theta \sim M(S), \quad H_1 : \theta \sim M(S'), \quad (3)$$

where the MIA is modelled as a test  $\phi : \Theta \rightarrow [0, 1]$  that maps a given mechanism output  $\theta$  to the probability of the null hypothesis  $H_0$  being rejected. Dong et al. (2022) analyzes this hypothesis test through the trade-off between the achievable *false positive rate* (FPR)  $\alpha_\phi \triangleq \mathbb{E}_{M(S)}[\phi]$  and *false negative rate* (FNR)  $\beta_\phi \triangleq 1 - \mathbb{E}_{M(S')}[\phi]$ , where the expectations are taken over the coin flips in the mechanism. Dong et al. (2022) formalizes the *trade-off function* and defines  $f$ -DP as follows:

**Definition 2.3.** A *trade-off curve*  $T(M(S), M(S')) : [0, 1] \rightarrow [0, 1]$  represents the FNR of the most powerful attack at any given FPR level  $\alpha$ :

$$T(M(S), M(S'))(\alpha) = \inf\{\beta_\phi \mid \alpha_\phi \leq \alpha, \phi : \Theta \rightarrow [0, 1]\} \quad (4)$$

See Figure 2 for an illustration.

**Definition 2.4.** A mechanism  $M(\cdot)$  satisfies  $f$ -DP, where  $f$  is the trade-off curve for some other mechanism  $\tilde{M}(\cdot)$ , if for any  $S \simeq S'$  we have  $T(M(S), M(S')) \geq f$ .

We state the equivalence between  $(\varepsilon, \delta)$ -DP guarantees and  $f$ -DP guarantees.

**Proposition 2.5 (Dong et al. (2022)).** A mechanism  $M(\cdot)$  is  $(\varepsilon, \delta)$ -DP iff it is  $f$ -DP with

$$f(\alpha) = \max\{0, 1 - \delta - e^\varepsilon \alpha, e^{-\varepsilon} \cdot (1 - \delta - \alpha)\}. \quad (5)$$

Moreover, a mechanism  $M(\cdot)$  satisfies  $(\varepsilon(\delta), \delta)$ -DP for all  $\delta \in [0, 1]$  iff it is  $f$ -DP with

$$f(\alpha) = \sup_{\delta \in [0, 1]} \max\{0, 1 - \delta - e^{\varepsilon(\delta)} \alpha, e^{-\varepsilon(\delta)} \cdot (1 - \delta - \alpha)\}. \quad (6)$$

We overview two particular notions of attack risk under  $f$ -DP. Attack risks can be thought of as a summary statistic of the  $f(\cdot)$  curve.

**Advantage/Accuracy.** Wood et al. (2018) proposed\* to measure the attack risk as the maximum achievable attack accuracy. To avoid confusion with model accuracy, we use *advantage* over random guessing, which is the difference between the attack TPR  $1 - \beta_\phi$  and FNR  $\alpha_\phi$ :

$$\eta \triangleq \sup_{S \simeq S'} \sup_{\phi: \Theta \rightarrow [0, 1]} 1 - \beta_\phi - \alpha_\phi. \quad (7)$$

We note that  $\eta$  is a transformation of maximum attack accuracy  $\sup 1/2 \cdot (1 - \beta_\phi) + 1/2 \cdot (1 - \alpha_\phi)$ , where supremum is over  $S \simeq S'$  and  $\phi: \Theta \rightarrow [0, 1]$ . Moreover,  $\eta$  can be obtained from a fixed point  $\alpha^* = f(\alpha^*)$  of the  $f(\cdot)$  curve as  $1 - 2\alpha^*$ , and is bounded given an  $(\varepsilon, \delta)$ -DP guarantee:

**Proposition 2.6 (Kairouz et al. (2015)).** If a mechanism  $M(\cdot)$  is  $(\varepsilon, \delta)$ -DP, then we have:

$$\eta \leq \frac{e^\varepsilon - 1 + 2\delta}{e^\varepsilon + 1}. \quad (8)$$

**FPR/FNR Risk.** The second common notion of risk we consider is the FPR/FNR of attacks. Recent work (Carlini et al., 2022; Rezaei and Liu, 2021) has argued that MIAs are a relevant threat only when the attack true positive rate  $1 - \beta_\phi$  is high at low enough  $\alpha_\phi$ . As a concrete notion of risk, we thus consider minimum level of attack FNR  $\beta^*$  within an FPR region  $\alpha \in [0, \alpha^*]$ , where  $\alpha^*$  is some low value. This approach is analogous to the statistically significant p-values often found in the sciences. Following the scientific standards and Carlini et al. (2022), we consider  $\alpha^* \in \{0.01, 0.05, 0.1\}$ .

**Reconstruction Robustness.** Another privacy threat is the reconstruction of training data records (see, e.g., Balle et al., 2022a). Denoting by  $R(\theta; z)$  an attack that aims to reconstruct  $z$ , its success probability can be formalized as  $\rho \triangleq \Pr[\ell(z, R(\theta; z)) \leq \gamma]$  over  $\theta \sim M(S \cup \{z\})$ ,  $z \sim \pi$  for some loss function  $\ell: \mathbb{D}^2 \rightarrow \mathbb{R}$  and prior  $\pi$ . Kaissis et al. (2023a) showed that MIA error rates bound reconstruction success as  $\rho \leq 1 - f(\alpha_\gamma)$  for an appropriate choice of  $\alpha_\gamma$ . Therefore, we can directly interpret the FPR/FNR trade-off curve as a notion of robustness to reconstruction attacks.

### 2.3 Attack-Aware Noise Calibration

The standard practice in DP is to calibrate the noise scale  $\omega$  of a mechanism  $M_\omega(\cdot)$  to some target  $(\varepsilon^*, \delta^*)$ -DP guarantee, with  $\varepsilon^*$  from a recommended range, e.g.,  $\varepsilon^* \in [3, 10]$ , and  $\delta^*$  fixed to  $\delta^* < 1/n$ , as in Eq. (2). Then, the privacy guarantees provided by the chosen  $(\varepsilon^*, \delta^*)$  are interpreted by mapping these values to bounds on sensitivity and specificity (by Proposition 2.5) or advantage (by Proposition 2.6) of membership inference attacks. In this work, we show that if the goal is to provide an operational and interpretable privacy guarantee, this approach leads to unnecessarily pessimistic noise requirements and a deterioration in utility due to the intermediate step of setting  $(\varepsilon^*, \delta^*)$ . Then, we show that it is possible to skip this intermediate step by using

\*Wood et al. (2018) used *posterior belief*, which is equivalent to accuracy under uniform prior.

the hypothesis-testing interpretation of DP to *directly* calibrate noise to operational notions of privacy risk. In practice, this means replacing the constraint in Eq. (2) with an operational notion of risk:

$$\min_{\omega \in \Omega} \omega \quad \text{s.t. } \text{risk}_\omega \leq \text{threshold}^*. \quad (9)$$

Solving this optimization problem requires two components. First, a way to optimize  $\omega$  given a method to compute  $\text{risk}_\omega$ . As we assume that risk is monotonic in  $\omega$ , Eq. (9) can be solved via binary search (see, e.g., Paszke et al., 2019) using calls to the  $\text{risk}_\omega$  function to an arbitrary precision. Second, we need a way to compute  $\text{risk}_\omega$  for any value  $\omega$ . In the next section, we provide efficient methods for doing so for general DP mechanisms, including composed mechanisms such as DP-SGD, by extending the tight privacy analysis from Doroshenko et al. (2022) to computing  $f$ -DP. Having these methods, we instantiate Eq. (9) for the notions of risks introduced in Section 2.2.

### 3 Numeric Calibration to Attack Risks

In this section, we provide methods for calibrating DP mechanisms to the notions of privacy risk in Section 2.2. As a first step, we introduce the core technical building blocks: methods for evaluating advantage  $\eta_\omega$  and the trade-off curve  $f_\omega(\alpha)$  of a mechanism for a given value of  $\omega$ .

**Dominating Pairs and PLRVs.** We make use of two concepts, originally developed in the context of computing tight privacy profiles under composition: *dominating pairs* (Zhu et al., 2022) and *privacy loss random variables* (PLRV) (Dwork and Rothblum, 2016).

**Definition 3.1.** We say that a pair of distributions  $(P, Q)$  is a *dominating pair* for a mechanism  $M(\cdot)$  if for every  $\varepsilon \in \mathbb{R}$  and  $S \simeq S'$ , we have  $D_{e^\varepsilon}(M(S) \parallel M(S')) \leq D_{e^\varepsilon}(P \parallel Q)$ .

Importantly, a dominating pair also provides a lower bound on the trade-off curve of a mechanism:

**Proposition 3.2.** *If  $(P, Q)$  is a dominating pair for a mechanism  $M(\cdot)$ , then for all  $S \simeq S'$ :*

$$T(M(S), M(S')) \geq T(P, Q). \quad (10)$$

The proofs of this and all the following statements are in Appendix D. Proposition 3.2 implies that a mechanism  $M(\cdot)$  is  $f$ -DP with  $f = T(P, Q)$ . Next, we introduce privacy loss random variables, which provide a natural parameterization of the curve  $T(P, Q)$ .

**Definition 3.3.** Suppose that a mechanism  $M(\cdot)$  has a discrete-valued dominating pair  $(P, Q)$ . Then, we define *privacy loss random variables* (PLRVs)  $(X, Y)$  as  $Y \triangleq \log Q(o)/P(o)$ , with  $o \sim Q$ , and  $X \triangleq \log Q(o')/P(o')$  with  $o' \sim P$ .

We can now state the result which serves as a main building block for our calibration algorithms, and forms the main theoretical contribution of our work.

**Theorem 3.4** (Accounting for advantage and  $f$ -DP with PLRVs). *Suppose that a mechanism  $M(\cdot)$  has a discrete-valued dominating pair  $(P, Q)$  with associated PLRVs  $(X, Y)$ . Attack advantage  $\eta$  for this mechanism is bounded:*

$$\eta \leq \Pr[Y > 0] - \Pr[X > 0]. \quad (11)$$

Moreover, for any  $\tau \in \mathbb{R}$ ,  $\gamma \in [0, 1]$ , we have  $T(P, Q)(\alpha(\tau, \gamma)) = \beta(\tau, \gamma)$ , where:

$$\alpha(\tau, \gamma) = \Pr[X > \tau] + \gamma \Pr[X = \tau], \quad \beta(\tau, \gamma) = \Pr[Y \leq \tau] - \gamma \Pr[Y = \tau]. \quad (12)$$

We remark that similar results for the trade-off curve appear in (Zhu et al., 2022), though the  $\gamma$  terms are not included as the PLRVs  $(X, Y)$  are assumed to be continuous. In this work, we rely on the technique due to Doroshenko et al. (2022) (summarized in Appendix E), which *discretizes* continuous mechanisms such as the subsampled Gaussian in DP-SGD, and provides a dominating pair that is *discrete* and finitely supported over an evenly spaced grid. As the dominating pairs are discrete, the  $\gamma$  terms are non-zero and necessary to fully reconstruct the trade-off curve.

### 3.1 Advantage Calibration

First, we show how to instantiate Eq. (9) to calibrate noise to a target advantage  $\eta^* \in [0, 1]$ . Let  $\eta_\omega$  denote the advantage of the mechanism  $M_\omega(\cdot)$  as defined in Eq. (7):

$$\min_{\omega \in \Omega} \omega \quad \text{s.t.} \quad \eta_\omega \leq \eta^*. \quad (13)$$

Given the PLRVs  $(X_\omega, Y_\omega)$ , we can obtain a substantially tighter bound than converting  $(\varepsilon, \delta)$  guarantees using Proposition 2.6 under standard calibration. Specifically, Theorem 3.4 provides the following way to solve the problem:

$$\min_{\omega \in \Omega} \omega \quad \text{s.t.} \quad \Pr[Y_\omega > 0] - \Pr[X_\omega > 0] \leq \eta^* \quad (14)$$

We call this approach *advantage calibration*, and show how to practically ensure it in Algorithm 3 in the Appendix. Given a method for obtaining valid PLRVs  $X_\omega, Y_\omega$  for any  $\omega$ , advantage calibration is *guaranteed* to ensure bounded advantage, which follows by combining Proposition 3.2 and Theorem 3.4:

**Proposition 3.5.** *Given PLRVs  $(X_\omega, Y_\omega)$  of a discrete-valued dominating pair of a mechanism  $M_\omega(\cdot)$ , choosing  $\omega^*$  using Eq. (14) ensures  $\eta_{\omega^*} \leq \eta^*$ .*

**Utility Benefits.** We demonstrate how calibration for a given level of attack advantage can increase utility. As a mechanism to calibrate, we consider DP-SGD with  $p = 0.001$  subsampling rate,  $T = 10,000$  iterations, and assume that  $\delta^* = 10^{-5}$ . Our goal is to compare the noise scale  $\sigma$  obtained via advantage calibration to the standard approach.

As a baseline, we choose  $\sigma$  using standard calibration in Eq. (2), and convert the resulting  $(\varepsilon, \delta)$  guarantees to advantage using Proposition 2.6. We consider target values of advantage  $\eta^* \in [0.01, 0.25]$ . As we show in Figure 3a, for any target value of advantage, the direct calibration procedure enables to reduce the noise scale by up to  $2\times$ .

**Pitfalls of Calibrating for Advantage.** Calibration to a given level of membership advantage is a compelling idea due to the decrease in noise required to achieve the same level of attack risk. Despite this increase in utility, we caution that this approach comes with a deterioration of privacy guarantees other than maximum advantage. Calibrating for a given level of advantage can be particularly dangerous without understanding the risks, as it allows for *increased attack success* in the security-critical regime of low attack FPR (see Section 2.2). The next result quantifies this pitfall:

**Proposition 3.6** (Cost of advantage calibration). *Fix a dataset size  $n > 1$ , and a target level of attack advantage  $\eta^* \in (\delta^*, 1)$ , where  $\delta^* = 1/c \cdot n$  for some  $c > 1$ . For any  $0 < \alpha < 1 - \eta^*/2$ , there exists a DP mechanism for which the gap in FNR  $f_{\text{standard}}(\alpha)$  obtained with standard calibration for  $\varepsilon^*$  that ensures  $\eta \leq \eta^*$ , and FNR  $f_{\text{adv}}(\alpha)$  obtained with advantage calibration is lower bounded:*

$$\Delta\beta(\alpha) \triangleq f_{\text{standard}}(\alpha) - f_{\text{adv}}(\alpha) \geq \eta^* - \delta^* + 2\alpha \frac{\eta^*}{\eta^* - 1}. \quad (15)$$

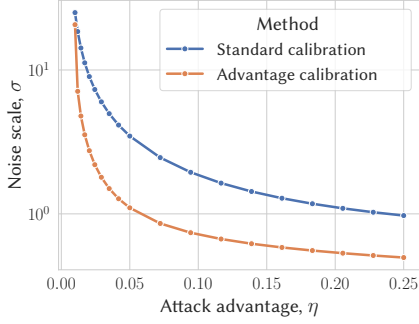
For example, if we aim to calibrate a mechanism to at most  $\eta^* = 0.5$  (or, 75% attack accuracy), we could potentially increase attack sensitivity by  $\Delta\beta(\alpha) \approx 30$  p.p. at FPR  $\alpha = 0.1$  compared to standard calibration with  $\delta^* = 10^{-5}$  (see the illustration in Figure 3b).

Note that the difference  $\Delta\beta$  in Proposition 3.6 is an overestimate of the actual harm due to advantage calibration for realistic mechanisms. Indeed, the increase in attack sensitivity can be significantly lower for mechanisms such as the Gaussian mechanism (see Figure 6 in the Appendix).

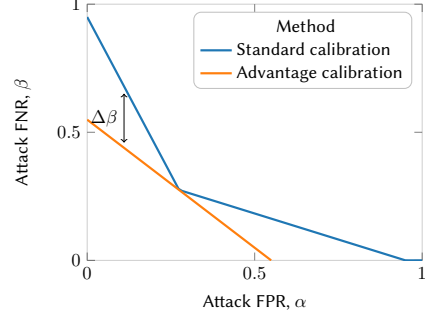
### 3.2 Safer Choice: Calibration to FNR within a Given FPR Region

In this section, we show how to calibrate the noise in any practical DP mechanism to a given minimum level of attack FNR  $\beta^*$  within an FPR region  $\alpha \in [0, \alpha^*]$ . We base this notion of risk off the previous work (Carlini et al., 2022; Rezaei and Liu, 2021) which argued that MIAs are a relevant threat only when the achievable TPR  $1 - \beta$  is high at low FPR  $\alpha$ . We instantiate the calibration problem in Eq. (9) as follows, assuming  $M_\omega(\cdot)$  satisfies  $f_\omega(\alpha)$ -DP:

$$\min_{\omega \in \Omega} \omega \quad \text{s.t.} \quad \inf_{0 \leq \alpha \leq \alpha^*} f_\omega(\alpha) \geq \beta^*. \quad (16)$$



(a) Calibrating noise to attack advantage significantly reduces the required noise scale compared to the standard approach. y axis is logarithmic.



(b) Optimal calibration for advantage comes with a pitfall: it allows for  $\Delta\beta$  higher attack power in the low FPR regime compared to standard calibration.

---

**Algorithm 1** Evaluate the Trade-Off Curve using Privacy Loss Random Variables  $(X, Y)$

---

**Require:** PMF  $\Pr[X_\omega = x_i]$  over grid  $\{x_1, x_2, \dots, x_k\}$  with  $x_1 < x_2 < \dots < x_k$

**Require:** PMF  $\Pr[Y_\omega = y_j]$  over grid  $\{y_1, y_2, \dots, y_l\}$  with  $y_1 < y_2 < \dots < y_l$

1: **procedure** COMPUTEFNR( $\omega; \alpha^*$ )

2:  $t \leftarrow \min\{i \in \{0, 1, \dots, k\} \mid \Pr[X_\omega > x_i] \leq \alpha^* < \Pr[X_\omega > x_{i-1}]\}$ , where  $x_0 \triangleq -\infty$

3:  $\gamma \leftarrow \frac{\alpha^* - \Pr[X_\omega > x_t]}{\Pr[X_\omega = x_t]}$

4: **return**  $f_\omega(\alpha^*) = \Pr[Y_\omega \leq x_t] - \gamma \Pr[Y_\omega = x_t]$

---

To solve Eq. (16), we begin by showing that such calibration is in fact equivalent to requiring a given level of attack FNR  $\beta^*$  and FPR  $\alpha^*$ .

**Proposition 3.7.** For any  $\alpha^* \geq 0, \beta^* \geq 0$  such that  $\alpha^* + \beta^* \leq 1$ , and any  $f$ -DP mechanism  $M(\cdot)$ :

$$\inf_{0 \leq \alpha \leq \alpha^*} f(\alpha) \geq \beta^* \text{ iff } f(\alpha^*) \geq \beta^*. \quad (17)$$

This follows directly by monotonicity of the trade-off function  $f$  (Dong et al., 2022). The optimization problem becomes:

$$\min_{\omega \in \Omega} \omega \text{ s.t. } f_\omega(\alpha^*) \geq \beta^*. \quad (18)$$

Unlike advantage calibration to  $\eta^*$ , the approach in Eq. (18) limits the adversary’s capabilities without risks in other regimes: They must compromise to achieve a lower FNR than  $\beta^*$  by testing at a higher FPR than  $\alpha^*$ , or, to achieve a lower FPR than  $\alpha^*$ , by testing at a higher FNR than  $\beta^*$ .

To obtain  $f_\omega(\alpha)$ , we use the PLRVs  $X_\omega, Y_\omega$  along with Theorem 3.4 to compute  $f = T(P, Q)$  (see Algorithm 1). We can then solve Eq. (18) using binary search over  $\Omega$  as mentioned in Section 2.3. Given a method that produces PLRVs  $X_\omega, Y_\omega$ , this algorithm *guarantees* the desired level of risk:

**Proposition 3.8.** Given PLRVs  $(X_\omega, Y_\omega)$  of a discrete-valued dominating pair of a mechanism  $M_\omega(\cdot)$ , choosing  $\omega^*$  using Eq. (18) and Algorithm 1 to compute  $f_\omega(\alpha)$  ensures  $f_{\omega^*}(\alpha^*) \geq \beta^*$ .

### 3.3 Other Approaches to Trade-Off Curve Accounting

In this section, we first contextualize the proposed method within existing work. Then, we discuss settings in which alternatives to PLRV-based procedures could be more suitable.

**Benefits of PLRV-based Trade-Off Curve Accounting.** Computational efficiency is important when estimating  $f_\omega(\alpha)$ , as the calibration problem requires evaluating this function multiple times for different values of  $\omega$  as part of binary search. Algorithm 1 computes  $f_\omega(\alpha)$  for a single  $\omega$  in  $\approx 500$ ms, enabling fast calibration, e.g., in  $\approx 1$  minute for DP-SGD with  $T = 10,000$  steps on commodity hardware (see Appendix F). Existing methods for estimating  $f_\omega(\alpha)$ , on the contrary, either provide weaker guarantees than Proposition 3.8 or are substantially less efficient. In particular, Dong et al. (2022) introduced  $\mu$ -GDP, an asymptotic expression for  $f_\omega(\alpha)$  as  $T \rightarrow \infty$ , that *overestimates* privacy (Gopi et al., 2021), and thus leads to mechanisms that do not satisfy the desired level of



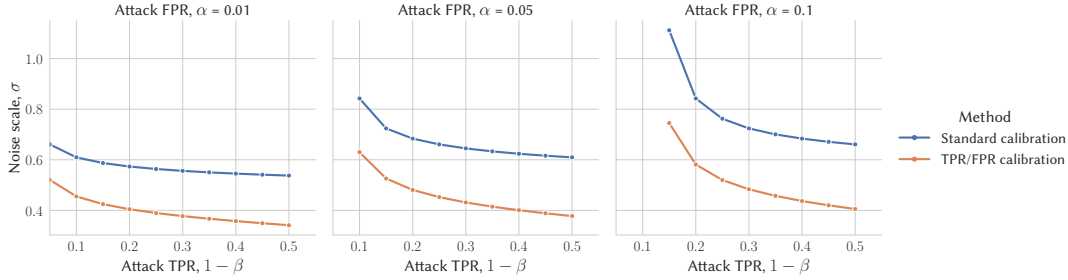


**Figure 4:** Calibration to attack TPR (i.e.,  $1 - \text{FNR}$ ) significantly reduces the noise scale in low FPR regimes. Unlike calibration for attack advantage, this approach does not come with a deterioration of privacy for low FPR, as it directly targets this regime.

attack resilience when calibrating to it. [Nasr et al. \(2023\)](#); [Zheng et al. \(2020\)](#) introduced a discretization-based approach to approximate  $f_\omega(\alpha)$  (discussed next) that can be orders of magnitude less efficient than the direct estimation in Algorithm 1, e.g., 1–6 minutes ( $\approx 100\text{--}700\times$  slower) for a single evaluation of  $f_\omega(\alpha)$  in the same setting as before, depending on the coarseness of discretization.

**Calibration using Black-Box Accountants.** Most DP mechanisms are accompanied by  $(\epsilon, \delta)$ -DP accountants, i.e., methods to compute their privacy profile  $\epsilon_\omega(\delta)$  or  $\delta_\omega(\epsilon)$ . Black-box access to these accountants enables to estimate  $\eta_\omega$  and  $f_\omega(\alpha)$ . In particular, Proposition 2.6 tells us that  $(0, \delta)$ -DP mechanisms bound advantage as  $\eta \leq \delta$ . Thus, advantage calibration can also be performed with any  $\epsilon_\omega(\delta)$  accountant by calibrating noise to ensure  $\epsilon_\omega(\eta^*) = 0$ . Estimating  $f_\omega(\alpha)$ , as mentioned previously, is less straightforward. Existing numeric approaches ([Nasr et al., 2023](#); [Zheng et al., 2020](#)) are equivalent to approximating Eq. (6) on a discrete grid over  $\delta \in \{\delta_1, \dots, \delta_u\}$ . This requires  $u$  calls to the accountant  $\epsilon_\omega(\delta)$ , thus quickly becomes inefficient for estimating  $f_\omega(\alpha)$  to high precision. We provide a detailed discussion of such black-box approaches in Appendix A.

**Calibration of Mechanisms with Known Trade-Off Curves.** An important advantage of our calibration methods is that they enable calibration of mechanisms whose privacy profile is unknown in the exact form, e.g., DP-SGD for  $T > 1$ . Simpler mechanisms, such as the Gaussian mechanism, which are used for simpler statistical analyses, e.g., private mean estimation, admit exact analytical solutions to the calibration problems in Eqs. (13) and (18). In Appendix B, we provide such solutions for the standard Gaussian mechanism, which enable efficient calibration without needing Algorithm 1.

## 4 Experiments

In this section, we aim to empirically evaluate the utility improvements of our calibration methods in simulations as well as in realistic applications.

**Simulations.** First, we demonstrate the noise reduction from calibrating for given error rates in the case of the DP-SGD algorithm using the setup in Section 3.1. We fix three low FPR regimes:  $\alpha^* \in \{0.01, 0.05, 0.1\}$ , and vary maximum attack sensitivity  $1 - \beta^*$  from 0.1 to 0.5 in each FPR regime. We show the results in Figure 4. We observe a significant decrease in the noise scale for all values. Although the decrease is less drastic than with calibration for advantage (see Figure 3a), in this case, we avoid the pitfalls of advantage calibration by directly calibrating for risk in the low FPR regime.

**Language Modeling and Image Classification.** We have showed that FNR/FPR calibration enables to significantly reduce the noise scale, but it is unclear how much of this reduction in noise translates into actual utility improvement in downstream applications. To answer this question, we evaluate our method for calibrating noise in private deep learning on two tasks: text sentiment classification using the SST-2 dataset ([Socher et al., 2013](#)), and image classification using the CIFAR-10 dataset ([Krizhevsky et al., 2009](#)).

For sentiment classification, we fine-tune GPT-2 (small) ([Radford et al., 2019](#)) using a DP version of LoRA ([Yu et al., 2021](#)). For image classification, we follow the approach of [Tramer and Boneh \(2021\)](#) of training a convolutional neural network on top of ScatterNet features ([Oyallon and Mallat, 2015](#)) with DP-SGD ([Abadi et al., 2016](#)). See additional details in Appendix F. For each setting, by varying the noise scale, we obtain several models at different levels of privacy. For each of the models we compute the guarantees in terms of TPR  $1 - \beta$  at three

fixed levels of FPR  $\alpha^* \in \{0.01, 0.05, 0.1\}$  that would be obtained under standard calibration, and using our Algorithm 1.

Figure 1 shows that FNR/FPR calibration enables to significantly increase *task* accuracy (a notion of utility; not to confuse with *attack* accuracy, a notion of privacy risk) at the same level of  $1 - \beta$  for all values of  $\alpha^*$ . For instance, for GPT-2, we see the accuracy increase of 18.3 p.p. at the same level of privacy risk (top leftmost plot).

## 5 Concluding Remarks

In this work, we proposed novel methods for calibrating noise in differentially private learning targeting a given level of operational privacy risk: advantage and FNR/FPR of membership inference attacks. Using simulations and end-to-end experiments, we showed that our calibration methods significantly decrease the required level of noise compared to the standard approach at the same level of operational risk. In the case of calibration for advantage, we also showed that the noise decrease could be harmful as it could allow for increased attack success in the low FPR regime, whereas calibration for a given level of FNR/FPR mitigates this issue. Next, we discuss limitations and possible directions for future work.

**Choice of Target FPR.** We leave open the question on how to choose the target FPR  $\alpha^*$ , e.g., whether standard significance levels in sciences such as  $\alpha^* = 0.05$  are compatible with data protection regulation. Future work is needed to develop concrete guidance on the choice of target FPR informed by legal and practical constraints.

**Tight Bounds for Privacy Auditing.** Multiple prior works on auditing the privacy properties of ML algorithms (Nasr et al., 2021; Liu et al., 2021; Jayaraman and Evans, 2019; Erlingsson et al., 2019) used conversions between  $(\epsilon, \delta)$  and operational risks like in Proposition 2.5, which we have shown to be loose for practical mechanisms. Beyond calibrating noise, our methods provide a tight and computationally efficient way of obtaining bounds on attack success rates for audits.

**Accounting in the Relaxed Threat Model.** Although we have focused on DP, our methods apply to any notion of privacy that is also formalized as a hypothesis test. In particular, our method can be used as is to compute privacy guarantees of DP-SGD in a relaxed threat model (RTM) proposed by Kaissis et al. (2023b). Previously, there was no efficient method for accounting in the RTM.

**Applications Beyond Privacy.** Our method can be applied to ensure provable generalization guarantees in deep learning. Indeed, prior work has shown that advantage  $\eta$  bounds generalization gaps of ML models (Kulynych et al., 2022). Thus, even though advantage calibration can exacerbate certain privacy risks, it can be a useful tool for ensuring a desired level of generalization in models that usually do not come with non-vacuous generalization guarantees, e.g., deep neural networks.

## References

- Martin Abadi, Andy Chu, Ian Goodfellow, H Brendan McMahan, Ilya Mironov, Kunal Talwar, and Li Zhang. Deep learning with differential privacy. In *Proceedings of the 2016 ACM SIGSAC conference on computer and communications security*, 2016.
- John Abowd and Ian Schmutte. Revisiting the economics of privacy: Population statistics and confidentiality protection as public goods. 2015.
- Wael Alghamdi, Shahab Asoodeh, Flavio P Calmon, Juan Felipe Gomez, Oliver Kosut, Lalitha Sankar, and Fei Wei. The saddle-point accountant for differential privacy. *arXiv preprint arXiv:2208.09595*, 2022.
- Borja Balle and Yu-Xiang Wang. Improving the gaussian mechanism for differential privacy: Analytical calibration and optimal denoising. In *International Conference on Machine Learning*. PMLR, 2018.
- Borja Balle, Giovanni Cherubin, and Jamie Hayes. Reconstructing training data with informed adversaries. In *2022 IEEE Symposium on Security and Privacy (SP)*, 2022a.
- Borja Balle, Giovanni Cherubin, and Jamie Hayes. Reconstructing training data with informed adversaries. In *2022 IEEE Symposium on Security and Privacy (SP)*. IEEE, 2022b.
- Nicholas Carlini, Steve Chien, Milad Nasr, Shuang Song, Andreas Terzis, and Florian Tramer. Membership inference attacks from first principles. In *2022 IEEE Symposium on Security and Privacy (SP)*, 2022.
- Kamalika Chaudhuri, Claire Monteleoni, and Anand D Sarwate. Differentially private empirical risk minimization. *Journal of Machine Learning Research*, 2011.
- Giovanni Cherubin, Boris Köpf, Andrew Paverd, Shruti Tople, Lukas Wutschitz, and Santiago Zanella-Béguelin. Closed-form bounds for DP-SGD against record-level inference. *arXiv preprint arXiv:2402.14397*, 2024.
- Rachel Cummings, Gabriel Kaptchuk, and Elissa M Redmiles. “I need a better description”: An investigation into user expectations for differential privacy. In *Proceedings of the 2021 ACM SIGSAC Conference on Computer and Communications Security*, 2021.
- Soham De, Leonard Berrada, Jamie Hayes, Samuel L Smith, and Borja Balle. Unlocking high-accuracy differentially private image classification through scale. *arXiv preprint arXiv:2204.13650*, 2022.
- Jinshuo Dong, Aaron Roth, and Weijie J Su. Gaussian differential privacy. *Journal of the Royal Statistical Society Series B: Statistical Methodology*, 2022.
- Vadym Doroshenko, Badih Ghazi, Pritish Kamath, Ravi Kumar, and Pasin Manurangsi. Connect the dots: Tighter discrete approximations of privacy loss distributions. *Proceedings on Privacy Enhancing Technologies*, 2022.
- Cynthia Dwork and Guy N Rothblum. Concentrated differential privacy. *arXiv preprint arXiv:1603.01887*, 2016.
- Cynthia Dwork, Frank McSherry, Kobbi Nissim, and Adam Smith. Calibrating noise to sensitivity in private data analysis. In *Proceedings of the Theory of Cryptography Conference*, 2006.
- Cynthia Dwork, Aaron Roth, et al. The algorithmic foundations of differential privacy. *Foundations and Trends in Theoretical Computer Science*, 2014.
- Úlfar Erlingsson, Ilya Mironov, Ananth Raghunathan, and Shuang Song. That which we call private. *arXiv preprint arXiv:1908.03566*, 2019.
- Daniel Franzen, Saskia Nuñez von Voigt, Peter Sörries, Florian Tschorsch, and Claudia Müller-Birn. Am i private and if so, how many? communicating privacy guarantees of differential privacy with risk communication formats. In *Proceedings of the 2022 ACM SIGSAC Conference on Computer and Communications Security*, 2022.
- Matt Fredrikson, Somesh Jha, and Thomas Ristenpart. Model inversion attacks that exploit confidence information and basic countermeasures. In *Proceedings of the ACM SIGSAC conference on computer and communications security*, 2015.

- Elena Ghazi and Ibrahim Issa. Total variation with differential privacy: Tighter composition and asymptotic bounds. In *IEEE International Symposium on Information Theory (ISIT)*, 2023.
- Sivakanth Gopi, Yin Tat Lee, and Lukas Wutschitz. Numerical composition of differential privacy. *Advances in Neural Information Processing Systems (NeurIPS)*, 2021.
- Charles R. Harris, K. Jarrod Millman, Stéfan J. van der Walt, Ralf Gommers, Pauli Virtanen, David Cournapeau, Eric Wieser, Julian Taylor, Sebastian Berg, Nathaniel J. Smith, Robert Kern, Matti Picus, Stephan Hoyer, Marten H. van Kerkwijk, Matthew Brett, Allan Haldane, Jaime Fernández del Río, Mark Wiebe, Pearu Peterson, Pierre Gérard-Marchant, Kevin Sheppard, Tyler Reddy, Warren Weckesser, Hameer Abbasi, Christoph Gohlke, and Travis E. Oliphant. Array programming with NumPy. *Nature*, 2020.
- Jamie Hayes, Borja Balle, and Saeed Mahloujifar. Bounding training data reconstruction in DP-SGD. *Advances in Neural Information Processing Systems*, 2024.
- Justin Hsu, Marco Gaboardi, Andreas Haeberlen, Sanjeev Khanna, Arjun Narayan, Benjamin C Pierce, and Aaron Roth. Differential privacy: An economic method for choosing epsilon. In *2014 IEEE 27th Computer Security Foundations Symposium*, 2014.
- Edward J Hu, Phillip Wallis, Zeyuan Allen-Zhu, Yuanzhi Li, Shean Wang, Lu Wang, Weizhu Chen, et al. Lora: Low-rank adaptation of large language models. In *International Conference on Learning Representations*, 2021.
- Zachary Izzo, Jinsung Yoon, Sercan O Arik, and James Zou. Provable membership inference privacy. *arXiv preprint arXiv:2211.06582*, 2022.
- Bargav Jayaraman and David Evans. Evaluating differentially private machine learning in practice. In *28th USENIX Security Symposium (USENIX Security 19)*, 2019.
- Bargav Jayaraman, Lingxiao Wang, Katherine Knipmeyer, Quanquan Gu, and David Evans. Revisiting membership inference under realistic assumptions. *Proceedings on Privacy Enhancing Technologies*, 2021.
- Richeng Jin, Zhonggen Su, cajiun zhong, Zhaoyang Zhang, Tony Quek, and Huaiyu Dai. Breaking the communication-privacy-accuracy tradeoff with f-differential privacy. *Advances in Neural Information Processing Systems (NeurIPS)*, 2023.
- Peter Kairouz, Sewoong Oh, and Pramod Viswanath. The composition theorem for differential privacy. In *International conference on machine learning*. PMLR, 2015.
- Georgios Kaissis, Jamie Hayes, Alexander Ziller, and Daniel Rueckert. Bounding data reconstruction attacks with the hypothesis testing interpretation of differential privacy. *arXiv preprint arXiv:2307.03928*, 2023a.
- Georgios Kaissis, Alexander Ziller, Stefan Kolek, Anneliese Riess, and Daniel Rueckert. Optimal privacy guarantees for a relaxed threat model: Addressing sub-optimal adversaries in differentially private machine learning. *Advances in Neural Information Processing Systems (NeurIPS)*, 2023b.
- Thomas Kluyver, Benjamin Ragan-Kelley, Fernando Pérez, Brian Granger, Matthias Bussonnier, Jonathan Frederic, Kyle Kelley, Jessica Hamrick, Jason Grout, Sylvain Corlay, Paul Ivanov, Damián Avila, Safia Abdalla, Carol Willing, and Jupyter development team. Jupyter notebooks - a publishing format for reproducible computational workflows. In *Positioning and Power in Academic Publishing: Players, Agents and Agendas*. IOS Press, 2016.
- Alex Krizhevsky, Geoffrey Hinton, et al. Learning multiple layers of features from tiny images. *Technical report*, 2009.
- Bogdan Kulynych, Yao-Yuan Yang, Yaodong Yu, Jaroslaw Blasiok, and Preetum Nakkiran. What you see is what you get: Principled deep learning via distributional generalization. *Advances in Neural Information Processing Systems (NeurIPS)*, 2022.
- Tobias Leemann, Martin Pawelczyk, and Gjergji Kasneci. Gaussian membership inference privacy. *Advances in Neural Information Processing Systems*, 36, 2024.
- Erich L Lehmann and Joseph P Romano. *Testing statistical hypotheses*. Springer Science & Business Media, 2006.

- Jiaxiang Liu, Simon Oya, and Florian Kerschbaum. Generalization techniques empirically outperform differential privacy against membership inference. *arXiv preprint arXiv:2110.05524*, 2021.
- Saeed Mahloujifar, Alexandre Sablayrolles, Graham Cormode, and Somesh Jha. Optimal membership inference bounds for adaptive composition of sampled gaussian mechanisms. *arXiv preprint arXiv:2204.06106*, 2022.
- Luise Mehner, Saskia Nuñez von Voigt, and Florian Tschorsch. Towards explaining epsilon: A worst-case study of differential privacy risks. In *2021 IEEE European Symposium on Security and Privacy Workshops (EuroS&PW)*, 2021.
- Priyanka Nanayakkara, Johes Bater, Xi He, Jessica Hullman, and Jennie Rogers. Visualizing privacy-utility trade-offs in differentially private data releases. *arXiv preprint arXiv:2201.05964*, 2022.
- Priyanka Nanayakkara, Mary Anne Smart, Rachel Cummings, Gabriel Kaptchuk, and Elissa M Redmiles. What are the chances? explaining the epsilon parameter in differential privacy. In *32nd USENIX Security Symposium (USENIX Security 23)*, 2023.
- Milad Nasr, Shuang Songi, Abhradeep Thakurta, Nicolas Papernot, and Nicholas Carlin. Adversary instantiation: Lower bounds for differentially private machine learning. In *IEEE Symposium on security and privacy (SP)*, 2021.
- Milad Nasr, Jamie Hayes, Thomas Steinke, Borja Balle, Florian Tramèr, Matthew Jagielski, Nicholas Carlini, and Andreas Terzis. Tight auditing of differentially private machine learning. In *32nd USENIX Security Symposium (USENIX Security 23)*, 2023.
- Kobbi Nissim, Salil Vadhan, and David Xiao. Redrawing the boundaries on purchasing data from privacy-sensitive individuals. In *Proceedings of the conference on Innovations in theoretical computer science*, 2014.
- Edouard Oyallon and Stéphane Mallat. Deep roto-translation scattering for object classification. In *Proceedings of the IEEE Conference on Computer Vision and Pattern Recognition*, 2015.
- The pandas development team. *pandas-dev/pandas: Pandas*, 2020.
- Adam Paszke, Sam Gross, Francisco Massa, Adam Lerer, James Bradbury, Gregory Chanan, Trevor Killeen, Zeming Lin, Natalia Gimelshein, Luca Antiga, et al. Pytorch: An imperative style, high-performance deep learning library. In *Advances in Neural Information Processing Systems (NeurIPS)*, 2019.
- Yury Polyanskiy and Yihong Wu. Information theory: From coding to learning. *Book draft*, 2022.
- Natalia Ponomareva, Hussein Hazimeh, Alex Kurakin, Zheng Xu, Carson Denison, H. Brendan McMahan, Sergei Vassilvitskii, Steve Chien, and Abhradeep Guha Thakurta. How to dp-fy ml: A practical guide to machine learning with differential privacy. *Journal of Artificial Intelligence Research*, 2023.
- Alec Radford, Jeffrey Wu, Rewon Child, David Luan, Dario Amodei, Ilya Sutskever, et al. Language models are unsupervised multitask learners. *OpenAI blog*, 2019.
- Shahbaz Rezaei and Xin Liu. On the difficulty of membership inference attacks. In *Proceedings of the IEEE/CVF Conference on Computer Vision and Pattern Recognition*, 2021.
- Tom Sander, Pierre Stock, and Alexandre Sablayrolles. TAN without a burn: Scaling laws of DP-SGD. In *Proceedings of the 40th International Conference on Machine Learning*, 2023.
- Reza Shokri, Marco Stronati, Congzheng Song, and Vitaly Shmatikov. Membership inference attacks against machine learning models. In *2017 IEEE symposium on security and privacy (SP)*. IEEE, 2017.
- Richard Socher, Alex Perelygin, Jean Wu, Jason Chuang, Christopher D. Manning, Andrew Ng, and Christopher Potts. Recursive deep models for semantic compositionality over a sentiment treebank. In *Proceedings of the 2013 Conference on Empirical Methods in Natural Language Processing*, 2013.
- Florian Tramèr and Dan Boneh. Differentially private learning needs better features (or much more data). In *International Conference on Learning Representations*, 2021.

- Pauli Virtanen, Ralf Gommers, Travis E. Oliphant, Matt Haberland, Tyler Reddy, David Cournapeau, Evgeni Burovski, Pearu Peterson, Warren Weckesser, Jonathan Bright, Stéfan J. van der Walt, Matthew Brett, Joshua Wilson, K. Jarrod Millman, Nikolay Mayorov, Andrew R. J. Nelson, Eric Jones, Robert Kern, Eric Larson, C J Carey, İlhan Polat, Yu Feng, Eric W. Moore, Jake VanderPlas, Denis Laxalde, Josef Perktold, Robert Cimrman, Ian Henriksen, E. A. Quintero, Charles R. Harris, Anne M. Archibald, Antônio H. Ribeiro, Fabian Pedregosa, Paul van Mulbregt, and SciPy 1.0 Contributors. SciPy 1.0: Fundamental Algorithms for Scientific Computing in Python. *Nature Methods*, 2020.
- Alex Wang, Amanpreet Singh, Julian Michael, Felix Hill, Omer Levy, and Samuel Bowman. Glue: A multi-task benchmark and analysis platform for natural language understanding. In *Proceedings of the 2018 EMNLP Workshop BlackboxNLP: Analyzing and Interpreting Neural Networks for NLP*, 2018.
- Michael L. Waskom. seaborn: statistical data visualization. *Journal of Open Source Software*, 6(60), 2021. doi: 10.21105/joss.03021. URL <https://doi.org/10.21105/joss.03021>.
- Larry Wasserman and Shuheng Zhou. A statistical framework for differential privacy. *Journal of the American Statistical Association*, 2010.
- Thomas Wolf, Lysandre Debut, Victor Sanh, Julien Chaumond, Clement Delangue, Anthony Moi, Pierric Cistac, Tim Rault, Rémi Louf, Morgan Funtowicz, et al. Huggingface’s transformers: State-of-the-art natural language processing. *arXiv preprint arXiv:1910.03771*, 2019.
- Alexandra Wood, Micah Altman, Aaron Bembenek, Mark Bun, Marco Gaboardi, James Honaker, Kobbi Nissim, David R O’Brien, Thomas Steinke, and Salil Vadhan. Differential privacy: A primer for a non-technical audience. *Vand. J. Ent. & Tech. L.*, 2018.
- Lukas Wutschitz, Huseyin A. Inan, and Andre Manoel. dp-transformers: Training transformer models with differential privacy. <https://www.microsoft.com/en-us/research/project/dp-transformers>, August 2022.
- Samuel Yeom, Irene Giacomelli, Matt Fredrikson, and Somesh Jha. Privacy risk in machine learning: Analyzing the connection to overfitting. In *2018 IEEE 31st Computer Security Foundations Symposium (CSF)*. IEEE, 2018.
- Ashkan Yousefpour, Igor Shilov, Alexandre Sablayrolles, Davide Testuggine, Karthik Prasad, Mani Malek, John Nguyen, Sayan Ghosh, Akash Bharadwaj, Jessica Zhao, Graham Cormode, and Ilya Mironov. Opacus: User-friendly differential privacy library in PyTorch. *arXiv preprint arXiv:2109.12298*, 2021.
- Da Yu, Saurabh Naik, Arturs Backurs, Sivakanth Gopi, Huseyin A Inan, Gautam Kamath, Janardhan Kulkarni, Yin Tat Lee, Andre Manoel, Lukas Wutschitz, et al. Differentially private fine-tuning of language models. In *International Conference on Learning Representations*, 2021.
- Qinqing Zheng, Jinshuo Dong, Qi Long, and Weijie Su. Sharp composition bounds for gaussian differential privacy via Edgeworth expansion. In *International Conference on Machine Learning*. PMLR, 2020.
- Yuqing Zhu, Jinshuo Dong, and Yu-Xiang Wang. Optimal accounting of differential privacy via characteristic function. In *Proceedings of The 25th International Conference on Artificial Intelligence and Statistics*, 2022.

## A Attack-Aware Noise Calibration with Black-box DP Accountants

**Advantage Calibration.** Proposition 2.6 implies that  $(0, \delta)$ -DP mechanisms ensure bounded advantage  $\eta \leq \delta$ . Therefore, given access to a black-box accountant  $\varepsilon_\omega(\delta)$  or  $\delta_\Omega(\varepsilon)$  we can calibrate to a given level of advantage  $\eta^*$  by ensuring  $(0, \eta^*)$ -DP:

$$\min_{\omega \in \Omega} \omega \quad \text{s.t.} \quad \varepsilon_\omega(\eta^*) = 0 \quad \text{or} \quad \delta_\omega(0) = \eta^* \quad (19)$$

This is a more generic way to perform advantage calibration using an arbitrary black-box accountant. It is equivalent to our procedure in Section 3.1 when using Doroshenko et al. (2022) accountant.

**FPR/FNR Calibration with Grid Search.** Given a black-box DP accountant, i.e., a method which computes the privacy profile  $\varepsilon_\omega(\delta)$  of a mechanism  $M_\omega(\cdot)$ , we can approximate  $f_\omega(\alpha)$  by discretizing the range of  $\delta \in [0, 1]$  and solving Eq. (6) as:

$$f_\omega(\alpha) \geq \sup_{\delta \in \{\delta_1, \delta_2, \dots, \delta_u\}} \max\{0, 1 - \delta - e^{\varepsilon_\omega(\delta)}\alpha, e^{-\varepsilon_\omega(\delta)} \cdot (1 - \delta - \alpha)\}, \quad (20)$$

where  $0 \leq \delta_1 < \delta_2 < \dots < \delta_u \leq 1$ . It is possible to perform an analogous discretization using  $\delta_\omega(\varepsilon)$  and Proposition D.1, in which case we have to additionally choose a bounded subspace  $\varepsilon \in [\varepsilon_{\min}, \varepsilon_{\max}] \subset \mathbb{R}$ . Equivalent procedures to Eq. (20) have previously appeared in Nasr et al. (2023); Zheng et al. (2020).

Plugging in Eq. (20) into the problem in Eq. (18), we can calibrate mechanisms to a given  $\alpha^*, \beta^*$  using binary search (see Section 2.3) in a space  $[\omega_{\min}, \omega_{\max}] \subseteq \Omega$  to additive error  $\omega_{\text{err}} > 0$ . Denoting by  $\nu$ :

$$\nu \triangleq \frac{\omega_{\max} - \omega_{\min}}{\omega_{\text{err}}}, \quad (21)$$

the calibration requires  $u \cdot \lceil \log_2 \nu \rceil$  evaluations of  $\varepsilon_\omega(\delta)$ . For instance, a single evaluation of the bound in Eq. (20) takes approximately one minute with  $u = 100$ , and six minutes with  $u = 1,000$  for DP-SGD with  $T = 10,000$  using Gopi et al. (2021) accountant as an instantiation of  $\varepsilon_\omega(\delta)$  on commodity hardware (see Appendix F). In contrast, evaluating  $f_\omega(\cdot)$  using Algorithm 1 in the same settings takes approximately 500ms at the default discretization level  $\Delta = 10^{-4}$  (see Appendix E).

Although this approach is substantially less computationally efficient than our direct procedure in Section 3.2, its strength is that it can be used to calibrate noise in any DP algorithm which provides a way to compute its  $(\varepsilon, \delta)$  guarantees.

## B Calibrating Gaussian Mechanism

In the case where the trade-off curve of the mechanism has a closed form, we can solve the calibration problems in Eqs. (13) and (18) exactly without resorting to the numerical procedures in Sections 3.1 and 3.2.

**Definition B.1.** For a given non-private algorithm  $q : 2^{\mathbb{D}} \rightarrow \mathbb{R}^d$ , a Gaussian mechanism (GM) is defined as  $M(S) = q(S) + \xi$ , where  $\xi \sim \mathcal{N}(0, \Delta_2 \cdot \sigma^2 \cdot I_d)$  and  $\Delta_2 \triangleq \sup_{S \sim S'} \|q(S) - q(S')\|_2$  is the *sensitivity* of  $q(S)$ .

For the Gaussian mechanism, we can exactly compute the relevant adversary's error rates:

**Proposition B.2** (Balle and Wang (2018); Dong et al. (2022)). *Suppose that  $M_\sigma(S)$  is GM with sensitivity  $\Delta_2$  and noise variance  $\sigma^2$ . Denote by  $\mu = \Delta_2/\sigma$  and by  $\Phi(t)$  the CDF of the standard Gaussian distribution  $\mathcal{N}(0, 1)$ . Then,*

- The mechanism satisfies  $(\varepsilon, \delta)$ -DP if the following holds:

$$\delta = \Phi\left(\frac{\mu}{2} - \frac{\varepsilon}{\mu}\right) - e^\varepsilon \Phi\left(-\frac{\mu}{2} - \frac{\varepsilon}{\mu}\right) \quad (22)$$

- It satisfies  $f$ -DP with:

$$f(\alpha) = \Phi\left(\Phi^{-1}(1 - \alpha) - \mu\right) \quad (23)$$

With these closed-form expressions, we can solve the calibration problems exactly:

**Corollary B.3** (Advantage calibration for GM). *For a GM  $M_\sigma(S)$  and target  $\eta^* > 0$ , choosing  $\sigma$  as:*

$$\sigma = \frac{\Delta_2}{2\Phi^{-1}\left(\frac{\eta^*+1}{2}\right)} \quad (24)$$

*ensures that adversary's advantage is upper bounded by  $\eta^*$ .*

*Proof of Corollary B.3.* It is sufficient to ensure  $(0, \eta^*)$ -DP. Plugging in  $\varepsilon = 0$  and  $\delta = \eta^*$  into Eq. (22), we have:

$$\eta^* = \Phi\left(\frac{\mu}{2}\right) - \Phi\left(-\frac{\mu}{2}\right) = 2\Phi\left(\frac{\mu}{2}\right) - 1, \quad (25)$$

from which we can derive  $\mu = \frac{\Delta_2}{\sigma} = 2\Phi^{-1}\left(\frac{\eta^*+1}{2}\right)$   $\square$

By solving Eq. (23) for  $\alpha$ , we also have an exact expression for calibrating to a given level of  $\alpha^*, \beta^*$ :

**Corollary B.4** (FPR/FNR calibration for GM). *For a Gaussian mechanism  $M_\sigma(S)$ , and target  $\alpha^* \geq 0, \beta^* \geq 0$  such that  $\alpha^* + \beta^* \leq 1$ , choosing  $\sigma$  as:*

$$\sigma = \frac{\Delta_2}{\Phi^{-1}(1 - \alpha^*) - \Phi^{-1}(\beta^*)} \quad (26)$$

*ensures that adversary's FNR and FPR rates are lower bounded by  $\alpha^*$  and  $\beta^*$ , respectively.*

Note that using the exact expressions above to calibrate Gaussian mechanism offer only computational advantages compared the method in the main body. In terms of resulting noise scale  $\sigma$ , the results are the same as with generic PLRV-based calibration up to a numerical approximation error.

## C Calibration to Other Risk Notions

Noise calibration for a given FPR/FNR level can be seen as a basic building block to calibrate for other operational measures of risk that are functions of FPR  $\alpha$  and FNR  $\beta$ .

For instance, [Rezaei and Liu \(2021\)](#) propose to measure the risks of membership inference attacks in terms of accuracy  $\text{acc}$  and FPR  $\alpha$ , where:  $\text{acc}(\alpha, \beta) \triangleq 1/2 \cdot ((1 - \alpha) + (1 - \beta))$ . We can calibrate for a given level of accuracy  $\text{acc}^*$  and FPR  $\alpha^*$  using the method in Section 3.2 by solving the expression for accuracy for a given  $\beta^*$ .

[Jayaraman et al. \(2021\)](#) propose to measure positive predictive value, or precision, of attacks:

$$\text{ppv}(\alpha, \beta) \triangleq \frac{1 - \beta}{1 - \beta + \alpha}. \quad (27)$$

Although precision alone is not sufficient to determine the level of privacy, like with accuracy, we can calibrate for a given level of precision  $\text{ppv}^*$  and FPR  $\alpha^*$  by deriving the corresponding  $\beta^*$ .

We provide the exact conversions in Table 1. These enable practitioners to use the calibration method in Section 3.2 while reporting technically equivalent but potentially more interpretable measures, e.g., attack accuracy at a given FPR.

**Beyond FNR and FPR.** Another avenue of calibrating to other risk measures is by leveraging different notions of divergence between probability distributions  $M(S)$  and  $M(S')$  instead of the the hockeystick divergence in Section 2.1. For instance, using Hellinger distance, one could model the success of membership inference attacks in which the attacker is given not a single observation as in Section 2.2, but countably many (see [Polyanskiy and Wu, 2022](#), Chapter 7). This, therefore, could capture risk with respect to practical repeated-observation attacks (e.g., [Jayaraman et al., 2021](#)).

## D Deferred Proofs

First, let us provide an analogous counterpart to Proposition 2.5:

**Proposition D.1.** *A mechanism  $M$  satisfies  $(\varepsilon, \delta(\varepsilon))$ -DP for all  $\varepsilon \in \mathbb{R}$  iff it is  $f$ -DP with*

$$f(\alpha) = \sup_{\varepsilon \in \mathbb{R}} \max\{0, 1 - \delta(\varepsilon) - e^\varepsilon \alpha, e^{-\varepsilon} \cdot (1 - \delta(\varepsilon) - \alpha)\}. \quad (28)$$



Attack risk measure	Symbol	Derived $\beta^*$
Advantage	$\eta^*$	$1 - \alpha^* - \eta^*$
Accuracy	$\text{acc}^*$	$2(\alpha^* - \text{acc}^*)$
Positive predictive value / precision	$\text{ppv}^*$	$\frac{(\alpha^* - 1)(\text{ppv}^* - 1)}{\text{ppv}^* - 1}$

**Table 1:** Some supported risk measures for calibration with a fixed level of FPR  $\alpha^*$ , with the derivation of the corresponding level of FNR  $\beta^*$ . Given  $\alpha^*$  and the derived  $\beta^*$ , we can calibrate noise using the procedure in Section 3.2.

*Proof of Proposition 3.2.* The result follows immediately from Proposition D.1 by plugging in  $D_{e^\varepsilon}(P \parallel Q)$  for  $\delta(\varepsilon)$ .  $\square$

*Proof of Proposition 3.6.* Let us fix a pair of datasets  $S \simeq S'$ , with  $|S| = n$ . Suppose that we have a mechanism  $M : 2^{\mathbb{D}} \rightarrow \{0, 1, 2, 3\}$  which satisfies  $(\varepsilon, \delta)$ -DP. Further, assume that for the specific fixed pair  $S, S'$  it is defined as follows:

$$\begin{aligned}
P(M(S) = 0) &= 0 & P(M(S') = 0) &= \delta \\
P(M(S) = 1) &= (1 - \delta) \cdot \frac{e^\varepsilon}{e^\varepsilon + 1} & P(M(S') = 1) &= (1 - \delta) \cdot \frac{1}{e^\varepsilon + 1} \\
P(M(S) = 2) &= (1 - \delta) \cdot \frac{1}{e^\varepsilon + 1} & P(M(S') = 2) &= (1 - \delta) \cdot \frac{e^\varepsilon}{e^\varepsilon + 1} \\
P(M(S) = 3) &= \delta & P(M(S') = 3) &= 0
\end{aligned} \tag{29}$$

The defining feature of this mechanism is that its trade-off curve  $T(M(S), M(S'))$  for  $S, S'$  exactly matches the  $f(\cdot)$  curve for generic  $(\varepsilon, \delta)$ -DP mechanisms in Eq. (5) (Kairouz et al., 2015). Thus, for this mechanism we can use  $f$  and  $T(M(S), M(S'))$  interchangeably. In the rest of the proof, we assume that we are calibrating this mechanism.

We want to derive (1)  $f_{\text{standard}}$  under standard calibration with  $\delta^* = 1/c \cdot n$  and  $\varepsilon^*$  chosen such that we have  $\eta \leq \eta^*$ , (2)  $f_{\text{adv}}$  under advantage calibration for ensuring  $\eta^*$ , and find their difference.

For this, we first solve Eq. (8) for  $\varepsilon$  to derive the corresponding  $\varepsilon^*$  that would satisfy the required level of  $\eta^*$  under standard calibration with  $\delta^* = \frac{1}{c \cdot n}$ :

$$\varepsilon^* = \log\left(\frac{2\delta^* - \eta^* - 1}{\eta^* - 1}\right) \tag{30}$$

As we are interested in the low  $\alpha$  regime, let us only consider the following form of the DP trade-off curve from Proposition 2.5:

$$f(\alpha) = 1 - \delta - e^\varepsilon \alpha. \tag{31}$$

It is easy to verify that this form holds for  $0 \leq \alpha \leq \frac{1-\delta}{1+e^\varepsilon}$ . In the case of  $(\varepsilon^*, \delta^*)$ -DP with  $\varepsilon^*$  defined by Eq. (30), a simple computation shows that this holds for  $0 \leq \alpha \leq \frac{1-\eta^*}{2}$ .

To get  $f_{\text{standard}}$ , we plug  $(\varepsilon^*, \delta^*)$  into the form in Eq. (31). Recall that by Eq. (8) advantage calibration for generic DP mechanisms is equivalent to calibrating noise to  $(0, \eta^*)$ -DP. Thus, to get  $f_{\text{adv}}(\alpha)$ , we plug in  $\varepsilon = 0, \delta = \eta^*$  to Eq. (31). Subtracting the two, we get:

$$\Delta\beta = \eta^* - \delta^* + 2\alpha \frac{\eta^* - \delta^*}{\eta^* - 1}, \tag{32}$$

from which we get the sought form.  $\square$

*Proof of Proposition 3.8.* Observe that Algorithm 1 returns the values of  $t, \tau$ , and  $\gamma$  considered in three cases of  $\alpha$  values in the proof of Theorem 3.4 given in Appendix D.1, and thus computes the valid trade-off curve  $T(P, Q)$  as defined in Eq. (12). By Proposition 3.2,  $M_\omega(\cdot)$  satisfies  $f$ -DP with  $f = T(P, Q)$ .  $\square$

## D.1 Proof of Theorem 3.4

Eq. (11) is an implication of a result by Gopi et al. (2021), which states:

$$\delta(\varepsilon) = \Pr[Y > \varepsilon] - e^\varepsilon \Pr[X > \varepsilon]. \tag{33}$$

We get Eq. (11) by observing that  $(0, \delta)$ -DP bounds  $\eta \leq \delta$  from Proposition 2.6.

In the remainder of the proof, we show Eq. (12). Let  $(P, Q)$  be a dominating pair as defined in Definition 3.1, and further let  $(P, Q)$  be discrete distributions with given pmfs, which we refer to as  $P(\cdot)$  and  $Q(\cdot)$ . We allow for multiple atoms  $o$  where  $P(o) > 0$  and  $Q(o) = 0$ , and also multiple atoms  $o'$  where  $Q(o') > 0$  and  $P(o') = 0$ . We make no further assumptions on  $(P, Q)$ . According to Neyman-Pearson (see, e.g., [Lehmann and Romano, 2006](#); [Dong et al., 2022](#)), the most powerful attack at level  $\alpha$  is a threshold test parameterized by two numbers  $\tau \in \mathbb{R}, \gamma \in [0, 1]$ .

$$\phi_{\tau, \gamma}^*(o) = \begin{cases} 1 & \text{if } \log \frac{Q(o)}{P(o)} > \tau \\ \gamma & \text{if } \log \frac{Q(o)}{P(o)} = \tau \\ 0 & \text{if } \log \frac{Q(o)}{P(o)} < \tau. \end{cases} \quad (34)$$

Intuitively,  $\phi$  outputs the probability that the sample  $o$  came from  $P$ ,  $\tau$  is the threshold of the test, and  $\log \frac{Q(o)}{P(o)}$  is our test statistic. If our test statistic happens to equal our threshold, we flip a coin with probability  $\gamma$  to determine if  $o$  came from  $Q$ .

We state the full scope of our proof. (1) we show that for any  $\tau \in \mathbb{R}$  and  $\gamma \in [0, 1]$ , one can use Eq. (12) to compute the trade-off function  $T(P, Q)$  at level  $\alpha^*(\tau, \gamma)$ , and (2) we show that the constraint  $\alpha^*(\tau, \gamma) = \alpha$  for any  $\alpha \in [0, 1]$  uniquely determines the optimal test  $\phi_{\tau, \gamma}^*$  that achieves the FPR  $\alpha$ . We start by proving (1). Recalling that  $X = \log Q(o)/P(o)$  with  $o \sim P$ , the FPR of  $\phi_{\tau, \gamma}^*(\theta)$  has the following form:

$$\alpha^*(\tau, \gamma) \triangleq \mathbb{E}_{\theta \sim P}[\phi_{\tau, \gamma}^*(\theta)] \quad (35)$$

$$= \Pr[X > \tau] + \gamma \Pr[X = \tau]. \quad (36)$$

Similarly,  $Y = \log Q(o)/P(o)$  with  $o \sim Q$ , the FNR of  $\phi_{\tau, \gamma}^*(\theta)$  has the following form:

$$\beta^*(\tau, \gamma) \triangleq 1 - \mathbb{E}_{\theta \sim Q}[\phi_{\tau, \gamma}^*(\theta)] \quad (37)$$

$$= 1 - (\Pr[Y > \tau] + \gamma \Pr[Y = \tau]) \quad (38)$$

$$= \Pr[Y \leq \tau] - \gamma \Pr[Y = \tau]. \quad (39)$$

These two equations parameterize the trade-off curve  $T(P, Q)$ .

We proceed to prove (2), i.e. that the constraint  $\alpha^*(\tau, \gamma) = \alpha$  for any  $\alpha \in [0, 1]$  uniquely determines the optimal test  $\phi_{\tau, \gamma}^*$  that achieves the FPR  $\alpha$ . Without loss of generality, we let  $X$  be supported over integers with mass at  $-\infty$ , i.e.  $\mathbb{X} \triangleq \{-\infty, 1, 2, \dots, k\} = \{x_0, \dots, x_k\}$ , with  $1 \leq k < \infty$ . The mass at  $-\infty$  is necessary because we allow for  $P$  to have non-zero mass at an atom  $o$  where  $Q$  has zero mass, leading to  $X = \log Q(o)/P(o) = -\infty$ . Indeed, this explicitly happens at  $o = -\infty$  in Algorithm 2. See Appendix E for more details.

Similarly, we let  $Y$  be supported over integers with mass at  $\infty$ , i.e.  $\mathbb{Y} \triangleq \{1, 2, \dots, l, \infty\} = \{x_1, \dots, x_{l+1}\}$ , with  $1 \leq l < \infty$ . The mass at  $\infty$  is necessary because we allow for  $Q$  to have non-zero mass at an atom  $o'$  where  $P$  has zero mass, leading to  $Y = \log Q(o')/P(o') = \infty$ .

We claim that the constraint  $\alpha^*(\tau, \gamma) = \alpha$  for any  $\alpha \in [0, 1]$  uniquely determines the optimal test  $\phi_{\tau, \gamma}^*$  that achieves the FPR  $\alpha$ . Moreover, the threshold  $\tau$  must be restricted to the domain of  $X$  without compromising on this uniqueness.

We begin by proving that  $\tau$  is restricted to the domain of  $X$ . We prove this by contradiction. Suppose there exists a  $\tau \notin \mathbb{X}$  such that  $\alpha^*(\tau, \gamma) = \alpha$  for any  $\alpha \in [0, 1]$ . We have that, for any  $\gamma$ :

$$\alpha^*(\tau, \gamma) = \Pr(X > \tau) + \gamma \Pr(X = \tau) \quad (40)$$

$$= \Pr(X > \tau) \quad (41)$$

$$= \Pr(X > \lceil \tau \rceil). \quad (42)$$

where Eq. (41) follows from the assumption that  $\tau \notin \mathbb{X}$ . Since  $X$  is a discrete random variable, Eq. (42) can only take on one of  $k + 1$  distinct values. If the level  $\alpha$  is not one of these  $k + 1$  values, then there is no choice of  $\tau$  and  $\gamma$  that can satisfy  $\alpha^*(\tau, \gamma) = \alpha$ , and a contradiction is reached.

Intuitively,  $\tau$  must be in the domain of  $X$ , as this is the only way for  $\gamma$  to have a non-zero impact on  $\alpha^*(\tau, \gamma)$ . Furthermore,  $\gamma$  is the only way for  $\alpha^*(\tau, \gamma)$  to take on values between the  $k + 1$  values of  $\Pr[X > x]$ ,  $x \in \mathbb{X}$ , which is necessary for the goal of having  $\alpha^*(\tau, \gamma)$  vary freely from  $[0, 1]$ .

Finally, we show that for any  $\tau$  in domain of  $X$  and  $\gamma \in [0, 1]$ , the constraint  $\alpha^*(\tau, \gamma) = \alpha$  for any  $\alpha \in [0, 1]$  uniquely determines the test  $\phi_{\tau, \gamma}$ . We break  $\alpha$  into three cases: (1) the edge case when  $\alpha = 1$ , (2) the case when

$\alpha < 1$  and  $\alpha$  coincides with the reverse CDF of  $X$ , i.e. there is a unique  $x_t \in \mathbb{X}$  such that  $\Pr(X > x_t) = \alpha$ , and (3) the regular case when  $\alpha < 1$  does not coincide with the reverse CDF of  $X$ .

**The Case of  $\alpha = 1$ .** We begin by noting that for fixed  $\gamma$ , the expression  $\alpha^*(\tau, \gamma)$  in Eq. (36) is monotonically decreasing in  $\tau$ , implying that  $\tau = -\infty$  maximizes Eq. (36) for any fixed  $\gamma$ . Moreover, for fixed  $\tau$ ,  $\alpha^*(\tau, \gamma)$  is monotonically increasing in  $\gamma$ , implying that  $\gamma = 1$  maximizes Eq. (36) for any fixed  $\tau$ . In this edge case, the only test that satisfies  $\alpha^*(\tau, \gamma) = 1$  is  $\tau = -\infty$  and  $\gamma = 1$ , and any other test achieves  $\alpha^* < 1$ . Moreover, since  $Y$  does not have mass at  $-\infty$ , the corresponding FNR for this Neyman-Pearson test, which is given by  $\beta^*(-\infty, 1)$  in Eq. (39), is 0.

**The Case of  $\alpha$  Coinciding with the Reverse CDF of  $X$ .** In this case,  $\alpha < 1$  and there is a unique  $x_t \in \mathbb{X}$  such that  $\Pr(X > x_t) = \alpha$ . We choose  $\tau$  to be  $x_t$  and  $\gamma = 0$ , since with these choices:

$$\alpha^*(x_t, \gamma = 0) = \Pr(X > x_t) \tag{43}$$

$$= \alpha. \tag{44}$$

In this case,  $\beta^*(\tau, \gamma)$  as defined in Eq. (39) is  $\Pr[Y \leq x_t]$ . Note that for  $t < k$ , we could just as easily have chosen  $\tau = x_{t+1}$  and  $\gamma = 1$  because:

$$\alpha^*(x_{t+1}, \gamma = 1) = \Pr(X > x_{t+1}) + \Pr(X = x_{t+1}) \tag{45}$$

$$= \Pr(X > x_t) \tag{46}$$

$$= \alpha. \tag{47}$$

And in this case,  $\beta^*(\tau, \gamma)$  as defined in Eq. (39) is  $\Pr[Y \leq x_{t+1}] - \Pr[Y = x_{t+1}] = \Pr[Y \leq x_t]$ . This means that either choice of  $\tau, \gamma$  yield the exact same test, as  $\phi_{x_t, 0}$  has an equivalent FNR and FPR to  $\phi_{x_{t+1}, 1}$ . This is the reason we distinguish this regime of  $\alpha$  from the other two regimes, as when  $\alpha$  is the reverse CDF of  $X$ , there are two ways to choose  $\tau, \gamma$  that yield the same Neyman-Pearson optimal test. This does not occur in the other regimes.

**The Case of  $\alpha$  not Coinciding with the Reverse CDF of  $X$ .** Finally, we investigate by far the most common regime, where  $\alpha$  is not 1 and also does not coincide with one of the  $k + 1$  values of the reverse CDF of the PLRV  $X$ . Here, we choose  $\tau$  to be  $x_t$ , the unique point in the domain of  $X$  whose reverse CDF values sandwich  $\alpha$ :

$$\alpha^*(x_t, \gamma = 0) < \alpha < \alpha^*(x_t, \gamma = 1). \tag{48}$$

and we choose  $\gamma$  to satisfy the constraint that  $\alpha^*(\tau, \gamma) = \alpha$ , i.e.,

$$\gamma = \frac{\alpha - \Pr[X > x_t]}{\Pr[X = x_t]}. \tag{49}$$

Note that  $\gamma \in (0, 1)$  in this case, and if we chose  $t$  to be any other index, it would be impossible to have  $\gamma \in [0, 1]$ .

This concludes our proof of (2), i.e. that the constraint  $\alpha^*(\tau, \gamma) = \alpha$  for any  $\alpha \in [0, 1]$  uniquely determines the optimal test  $\phi_{\tau, \gamma}^*$  that achieves the FPR  $\alpha$ .

We remark that similar results regarding the trade-off curve between two discrete mechanisms can be found in Jin et al. (2023). We differ from this work by parameterizing the trade-off curve using PLRVs, in contrast to Jin et al. (2023), who parameterized the trade-off curve in terms of the discrete distributions  $P$  and  $Q$ . Our parameterization lends itself more naturally to composition, as the PLRVs sum under composition.

## E Dominating Pairs

### E.1 Constructing Discrete Dominating Pairs and their PLRVs

We summarize the technique from Doroshenko et al. (2022) to construct a dominating pair from a composed mechanism  $M(S) = M^{(1)} \circ M^{(2)} \circ \dots \circ M^{(T)}(S)$ . This models the common use case in privacy-preserving ML where a simple mechanism, such as the subsampled Gaussian in DP-SGD, is applied  $T$  times. We assume that each sub-mechanism  $M^{(i)}$ ,  $i \in [T]$ , has a known privacy curve  $\delta_i(\varepsilon)$ . Given an input discretization parameter  $\Delta$ , a size  $k$ , and a starting  $\varepsilon_1$ , (Doroshenko et al., 2022) creates a grid  $\{\varepsilon_1, \varepsilon_1 + \Delta, \dots, \varepsilon_1 + k\Delta\}$ . Then, they compute the privacy curve on this grid  $\{\delta_i(\varepsilon_1), \delta_i(\varepsilon_1 + \Delta), \dots, \delta_i(\varepsilon_1 + k\Delta)\}$ , and append the values of  $\delta(-\infty) = 0$  and

---

**Algorithm 2** (Doroshenko et al., 2022) Construct Dominating Pair

---

**Require:** Grid:  $\{-\infty, \varepsilon_1, \dots, \varepsilon_k, \infty\}$ .

**Require:** Privacy curve on a grid:  $\{0, \delta(\varepsilon_1), \dots, \delta(\varepsilon_k), \delta(\infty)\}$ .

```
1:  $P(\infty) = 0$ 
2: for  $i = k - 1, \dots, 1$  do
3:    $P(\varepsilon_i) \leftarrow \frac{\delta(\varepsilon_{i-1}) - \delta(\varepsilon_i)}{\exp(\varepsilon_i) - \exp(\varepsilon_{i-1})} - \frac{\delta(\varepsilon_i) - \delta(\varepsilon_{i+1})}{\exp(\varepsilon_{i+1}) - \exp(\varepsilon_i)}$ 
4:  $P(-\infty) \leftarrow 1 - \sum_{j \in [k-1]} P(\varepsilon_j)$ 
5:  $Q(-\infty) \leftarrow 0$ 
6: for  $i = 1, \dots, k - 1$  do
7:    $Q(\varepsilon_i) \leftarrow \exp(\varepsilon_i) P(\varepsilon_i)$ 
8:  $Q(\infty) = \delta(\infty)$ 
9: return  $(P, Q)$ 
```

---

$\delta(\infty)$ . The dominating pair for the  $i^{\text{th}}$  mechanism is constructed using Algorithm 2. Note that Algorithm 2 is identical to Algorithm 1 in Doroshenko et al. (2022), with the notation modified to be consistent with the notation in this paper.

Notably, both  $P_i$  and  $Q_i$  have support on the discrete grid  $\{\exp(\varepsilon_1), \exp(\varepsilon_1 + \Delta), \dots, \exp(\varepsilon_1 + k\Delta)\}$ , though  $Q$  has support at  $\infty$  and  $P$  has support at  $-\infty$ . By construction, the PLRV  $Y$  has the same pmf as  $Q$  but support on the grid  $\{\varepsilon_1, \varepsilon_1 + \Delta, \dots, \varepsilon_1 + k\Delta, \infty\}$ . Similarly, PLRV  $X$  has the same pmf as  $P$  but support on  $\{-\infty, \varepsilon_1, \varepsilon_1 + \Delta, \dots, \varepsilon_1 + k\Delta\}$ .

This process is repeated for every mechanism. As long as the discretization parameter  $\Delta$  is the same for all  $T$  mechanisms, the resulting collection of PLRVs can be composed via the Fast Fourier Transform. The dominating pair for the composed mechanism  $M$  is simply the distribution of  $(X_1 + X_2 \dots + X_T, Y_1 + Y_2 \dots + Y_T)$ .

We remark that the discretization parameter  $\Delta$  is user-defined, and the choice for the size  $k$  and starting  $\varepsilon$  for each grid is mechanism-specific. For further implementation details, we point the reader to the code [documentation file](#) and the code itself, which can be found on Google’s differential privacy library. In particular, we note that while the PLRVs  $X, Y$  have the same support except for atoms at  $\pm\infty$ , the support of the composed PLRV  $X_1 + X_2 \dots + X_T$  need not be the same as the support of  $Y_1 + Y_2 \dots + Y_T$ . This is because in the convolution part of the implementation of Doroshenko et al. (2022), the code discards any tail probabilities smaller than some truncation parameter. This is why we allow for  $X$  and  $Y$  to have different support in Algorithm 1, and why we make no assumptions on the distributions of  $(P, Q)$  or of  $(X, Y)$  in the proof for Theorem 3.4.

## E.2 Some Properties of the Trade-Off Curves of Discrete Dominating Pairs

In this section, we provide several observations on the trade-off curve of discrete dominating pairs. In particular, these observations hold for the trade-off curve described Theorem 3.4.

**Connecting the Dots.** From the proof of Theorem 3.4 (see Appendix D.1), we know that when the level  $\alpha$  happens to equal a point in the reverse CDF of  $X$ , i.e. when  $\alpha = \Pr[X > x_i]$  for some  $i$ , that the corresponding FNR  $T(P, Q)(\alpha)$  is simply the CDF of  $Y$  evaluated at the same point, i.e.  $T(P, Q)(\alpha) = \Pr[Y \leq x_i]$ . Since the reverse CDF of  $X$  can take on  $k + 1$  values, it follows that there are  $k + 1$  values of  $\alpha$  where the trade-off curve is fully characterized by the CDF of the PLRVs.

Next, we observe a special structure of the trade-off curve on the points outside of these  $k + 1$  values. For fixed  $\tau$ , Eq. (36) implies  $\alpha^*(\tau, \gamma)$  is increasing linearly in  $\gamma$  and Eq. (39) implies  $\beta^*(\tau, \gamma)$  is decreasing linearly in  $\gamma$ . This implies that the trade-off curve “in between” the  $k + 1$  points that correspond to the CDFs of the PLRVs is a *linear interpolation*, where one “connects the dots”. Hence, the trade-off curve is piece-wise linear, continuous everywhere, and not differentiable at the  $k + 1$  points where  $\alpha$  happens to be on the reverse CDF of  $X$ .

This observation provides an interesting connection to Doroshenko et al. (2022), who similarly showed that “connecting the dots” between finite points on the *privacy profile*  $\delta(e^\varepsilon)$ <sup>†</sup> yields a valid privacy profile. We emphasize that the context is different: Doroshenko et al. (2022) showed that “connecting the dots” between *any* collection of finite points on the privacy profile yields a pessimistic privacy profile because “connecting the dots” corresponds the most pessimistic bound. This follows because “higher is less private” in privacy profile space, and because the privacy profile is convex, it follows that a linear interpolation is the least private the collection of

---

<sup>†</sup>The linear interpolation must be done in  $e^\varepsilon$  space, as in this grid the privacy profile  $\delta(e^\varepsilon)$  is convex.

---

**Algorithm 3** Evaluate Advantage using PLRVs  $(X, Y)$ 

---

**Require:** PMF  $\Pr[X_\omega = \tau]$  over grid  $\{x_1, x_2, \dots, x_k\}$  with  $x_1 < x_2 < \dots < x_k$

**Require:** PMF  $\Pr[Y_\omega = \tau]$  over grid  $\{y_1, y_2, \dots, y_l\}$  with  $y_1 < y_2 < \dots < y_l$

**Output:** Upper bound  $\eta^\uparrow$  such that  $\eta_\omega \leq \eta^\uparrow$

- 1: **procedure** COMPUTEADV( $\omega$ )
  - 2:    $t_X \leftarrow \min\{i \in [k] \mid x_i > 0\}, t_Y \leftarrow \min\{i \in [l] \mid y_i > 0\}$
  - 3:   **return**  $\eta^\uparrow = \sum_{i=t_Y}^l \Pr[Y_\omega = y_i] - \sum_{i=t_X}^k \Pr[X_\omega = x_i]$
- 

points on the privacy curve could be. In contrast, “connecting the dots” on the trade-off curve corresponds to the most optimistic bound, since the trade-off curve is convex and “higher is more private”, meaning “connecting the dots” is the most private the collection of points can be in general. However, as we detail before, discrete mechanisms in fact achieve this optimistic bound.

**Behavior at the Edges.** The trade-off curve of discrete dominating  $(P, Q)$  in general does not satisfy  $T(P, Q)(0) = 1$ . Indeed, the point  $\alpha = 0$  corresponds to  $\tau = x_k$  and  $\gamma = 0$ , in which case  $T(P, Q)(0) = \Pr[Y \leq x_k] = 1 - \Pr[Y > x_k]$ . Whether or not this equals 1 depends on the details of the PLRV  $Y$ , though we note that in our experiments,  $T(P, Q)(0)$  is usually 1 to within a margin of  $10^{-10}$ . Moreover, we have that  $T(P, Q)(\alpha) = 0$  for any  $\alpha \in [\Pr[X > -\infty], 1]$ . Indeed, for any  $\alpha \in [\Pr[X > -\infty], 1]$ , we have that  $\tau = -\infty$ , meaning that  $\beta^*(\tau, \gamma) = \Pr[Y \leq -\infty] = 0$  for any choice of  $\gamma$ .

The observation that  $T(P, Q)(0) \neq 1$ , that  $T(P, Q)$  is piece-wise linear, and that  $T(P, Q)(\alpha) = 0$  for any sufficiently large  $\alpha$ , are all consistent with the findings of Jin et al. (2023), who characterized the trade-off curves of discrete-valued mechanisms.

## F Additional Details and Figures

### F.1 Computing Resources

We use a commodity machine with AMD Ryzen 5 2600 six-core CPU, 16GB of RAM, and an Nvidia GeForce RTX 4070 GPU with 16GB of VRAM to run our experiments. All experiments with deep learning take up to four hours to finish.

### F.2 Experimental Setup

**Text Sentiment Classification.** We follow Yu et al. (2021) to finetune a GPT-2 (small) (Radford et al., 2019) using LoRA (Hu et al., 2021) with DP-SGD on the SST-2 sentiment classification task (Socher et al., 2013) from the GLUE benchmark (Wang et al., 2018). We use the batch size of 256, gradient clipping norm of  $\Delta_2 = 1.0$ , and finetune for three epochs with LoRA of dimension 4 and scaling factor of 32. We vary the noise multiplier  $\sigma \in \{0.5715, 0.6072, 0.6366, 0.6945, 0.7498\}$  approximately corresponding to  $\varepsilon \in \{3.95, 3.2, 2.7, 1.9, 1.45\}$ , respectively, at  $\delta = 10^{-5}$ . We use the default training split of the SST-2 dataset containing 67,348 examples for finetuning, and the default validation split containing 872 examples as a test set.

**Image Classification.** We follow Tramer and Boneh (2021) to train a convolutional neural network (Tramer and Boneh, 2021, Table 9, Appendix) over the ScatterNet features (Oyallon and Mallat, 2015) on the CIFAR-10 (Krizhevsky et al., 2009) image classification dataset. We use batch size of 8192, learning rate of 4, Nesterov momentum of 0.9, and gradient clipping norm of  $\Delta_2 = 0.1$ . We train for up to 100 epochs. We vary the gradient noise multiplier  $\sigma/\Delta_2 \in \{4, 5, 6, 8, 10\}$ , and use the Moments accountant (Abadi et al., 2016) to derive the  $(\varepsilon, \delta)$  privacy guarantees. As the privacy accounting in the setup of Tramer and Boneh (2021) requires accounting for a composition of DP-SGD and a data normalization step, we follow their accounting procedure which uses the Moments accountant (Abadi et al., 2016) unlike the other experiment. We use the default 50K/10K train/test split of CIFAR-10.

### F.3 Software

We use the following key open-source software:

- PyTorch ([Paszke et al., 2019](#)) for implementing neural networks.
- huggingface ([Wolf et al., 2019](#)) suite of packages for training language models.
- opacus ([Yousefpour et al., 2021](#)) for training PyTorch neural networks with DP-SGD.
- dp-transformers ([Wutschitz et al., 2022](#)) for differentially private finetuning of language models.
- numpy ([Harris et al., 2020](#)), scipy ([Virtanen et al., 2020](#)), pandas ([pandas development team, 2020](#)), and jupyter ([Kluyver et al., 2016](#)) for numeric analyses.
- seaborn ([Waskom, 2021](#)) for visualizations.

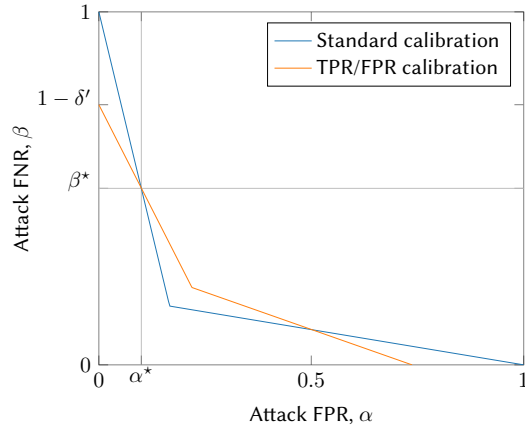


**Figure 5:** When calibrating a generic DP mechanism to a given level of attack TPR/FPR, the gain compared to standard calibration comes from a relatively high  $\delta'$  value. In this example, we aim to ensure that DP-SGD with  $T = 10,000$  iterations, sample rate  $p = 0.001$ , and  $n < 10^5$  has membership inference attack TPR bounded as  $1 - \beta^* \leq 0.5$  at FPR  $\alpha^* = 0.1$ . With standard calibration, we use  $\delta^* = 10^{-5}$ , and find that  $\varepsilon \approx 1.61$  satisfies the TPR/FPR requirement (blue trade-off curve). With direct calibration for  $\alpha^*, \beta^*$ , we find that we get the lowest noise scale  $\sigma'$  if we set  $\delta' \approx 0.263$  and  $\varepsilon' \approx 0.86$  (orange trade-off curve). If we were to run accounting for this noise scale at the standard  $\delta = 10^{-5}$ , we would get  $\varepsilon \approx 9.6$ .

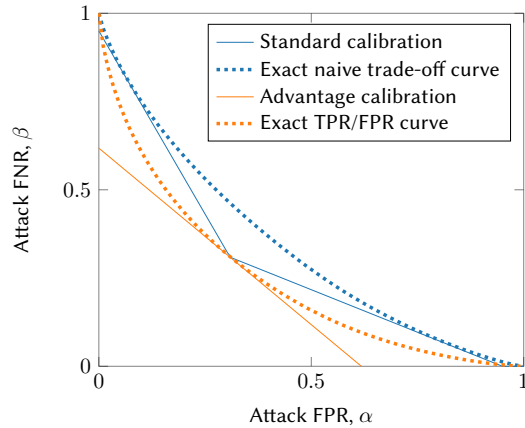


**Figure 6:** The increase in attack sensitivity due to calibration for advantage is less drastic for Gaussian mechanism than for a generic  $(\varepsilon, \delta)$ -DP mechanism. See Figure 5 for the details for the case of a generic mechanism.